

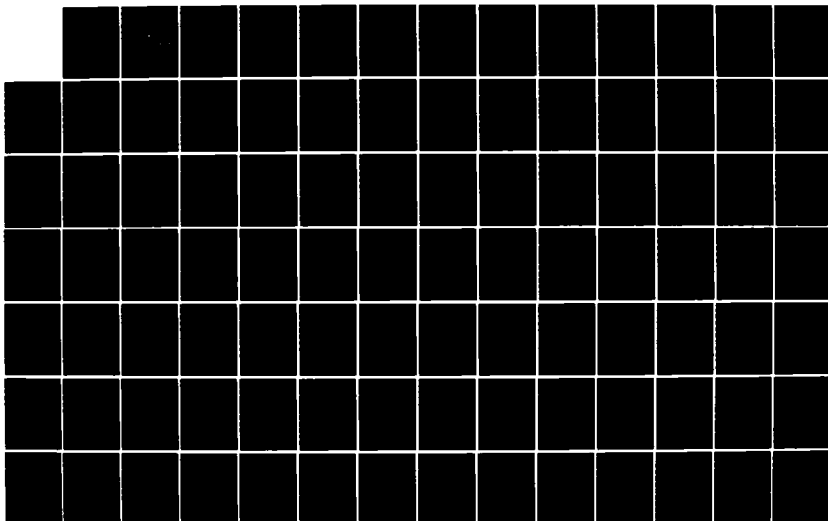
AD-A152 550

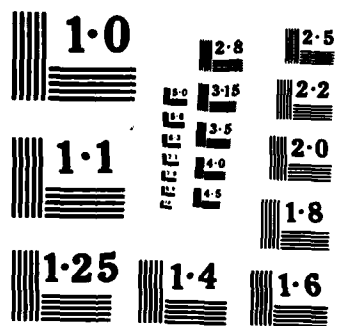
SPECTRAL DECOMPOSITION AND VERIFICATION OF NOGAPS 500MB 1/1  
MEDIUM-RANGE FORECASTS(U) NAVAL POSTGRADUATE SCHOOL  
MONTEREY CA R C SHONALTER SEP 84

UNCLASSIFIED

F/G 4/2

NL





2

# NAVAL POSTGRADUATE SCHOOL

Monterey, California

AD-A152 550



DTIC  
ELECTE  
APR 18 1985  
S E D

## THESIS

SPECTRAL DECOMPOSITION AND VERIFICATION  
OF NOGAPS 500MB MEDIUM-RANGE FORECASTS

by

Robert C. Showalter

September 1984

Thesis Co-advisors:

C. H. Wash  
J. S. Boyle

Approved for public release; distribution unlimited.

DTIC FILE COPY

00 0 2. 013

UNCLASSIFIED

SECURITY CLASSIFICATION OF THIS PAGE (When Data Entered)

REPORT DOCUMENTATION PAGE		READ INSTRUCTIONS BEFORE COMPLETING FORM
1. REPORT NUMBER	2. GOVT ACCESSION NO. <b>AD-A152</b>	3. RECIPIENT'S CATALOG NUMBER <b>560</b>
4. TITLE (and Subtitle) Spectral Decomposition and Verification of NOGAPS 500mb Medium-Range Forecasts		5. TYPE OF REPORT & PERIOD COVERED Master's Thesis; September 1984
7. AUTHOR(s) Robert C. Showalter		6. PERFORMING ORG. REPORT NUMBER
9. PERFORMING ORGANIZATION NAME AND ADDRESS Naval Postgraduate School Monterey, California 93943		8. CONTRACT OR GRANT NUMBER(s)
11. CONTROLLING OFFICE NAME AND ADDRESS Naval Postgraduate School Monterey, California 93943		10. PROGRAM ELEMENT, PROJECT, TASK AREA & WORK UNIT NUMBERS
14. MONITORING AGENCY NAME & ADDRESS (if different from Controlling Office)		12. REPORT DATE September 1984
		13. NUMBER OF PAGES 95
		15. SECURITY CLASS. (of this report) Unclassified
		15a. DECLASSIFICATION/DOWNGRADING SCHEDULE
16. DISTRIBUTION STATEMENT (of this Report)  Approved for public release; distribution unlimited.		
17. DISTRIBUTION STATEMENT (of the abstract entered in Block 20, if different from Report)		
18. SUPPLEMENTARY NOTES		
19. KEY WORDS (Continue on reverse side if necessary and identify by block number)  Numerical Weather Prediction Navy Operational Global Atmospheric Prediction System Spectral Decomposition Amplitude Smoothing		
20. ABSTRACT (Continue on reverse side if necessary and identify by block number)  Twelve NOGAPS 500mb 5-day forecasts were spectrally decomposed into wavenumber groupings for verification purposes. Four forecasts were from the NOGAPS 2.0 (six-level) version and eight from the NOGAPS 2.1 (nine-level) version. Wavenumber components of the forecast and observed waves were grouped into planetary (wavenumbers 1-3), long (wavenumbers 4-7) and medium (wavenumbers		

DD FORM 1473  
1 JAN 73EDITION OF 1 NOV 65 IS OBSOLETE  
S/N 0102-LF-014-6601

1

UNCLASSIFIED

SECURITY CLASSIFICATION OF THIS PAGE (When Data Entered)

UNCLASSIFIED

SECURITY CLASSIFICATION OF THIS PAGE (When Data Entered)

#20 - ABSTRACT - (CONTINUED)

8-12) to facilitate model comparison. Hovmoller (time-longitude) diagrams were used to analyze the observed and forecast fields.

Two systematic errors emerged; amplitude smoothing of wave and trough features, and consistent positive error at high latitudes. NOGAPS 2.1 demonstrated modest improvement (over NOGAPS 2.0) as error magnitudes were reduced and initiation of error occurred later in the forecast. Both NOGAPS 2.0 and NOGAPS 2.1 showed positive error growth near the poles and no improvement was noted in the newer model version.

S/N 0102- LF-014-6601

UNCLASSIFIED

SECURITY CLASSIFICATION OF THIS PAGE (When Data Entered)

Approved for public release; distribution unlimited.

Spectral Decomposition and Verification  
of NOGAPS 500mb Medium-Range Forecasts

by

Robert C. Showalter  
Lieutenant Commander, United States Navy  
B.S., Purdue University, 1973

Submitted in partial fulfillment of the  
requirements for the degree of

MASTER OF SCIENCE IN METEOROLOGY AND OCEANOGRAPHY

from the

NAVAL POSTGRADUATE SCHOOL

September 1984

Accession For	
NTIS GRA&I	<input checked="" type="checkbox"/>
DTIC TAB	<input type="checkbox"/>
Unannounced	<input type="checkbox"/>
Justification	
By	
Distribution/	
Availability Codes	
Distribution/	
Special	



A-1

Author:

*Robert C. Showalter*

Approved by:

*Clyde H. Work*

Co-advisor

*James S. Boyle*

Co-advisor

*Richard D. Miller*

Chairman, Department of Meteorology

*M. Dyer*

Dean of Science and Engineering

ABSTRACT

Twelve NOGAPS 500mb 5-day forecasts were spectrally decomposed into wavenumber groupings for verification purposes. Four forecasts were from the NOGAPS 2.0 (~~six~~-level) version and eight from the NOGAPS 2.1 (~~nine~~-level) version. Wavenumber components of the forecast and observed waves were grouped into planetary (wavenumbers 1-3), long (wavenumbers 4-7) and medium (wavenumbers 8-12) to facilitate model comparison. Hovmoller (time-longitude) diagrams were used to analyze the observed and forecast fields.

Two systematic errors emerged; amplitude smoothing of wave and trough features, and consistent positive error at high latitudes. NOGAPS 2.1 demonstrated modest improvement (over NOGAPS 2.0) as error magnitudes were reduced and initiation of error occurred later in the forecast. Both NOGAPS 2.0 and NOGAPS 2.1 showed positive error growth near the poles and no improvement was noted in the newer model version.

## TABLE OF CONTENTS

I.	INTRODUCTION -----	11
II.	NOGAPS SUMMARY AND SPECTRAL VERIFICATION APPROACH -----	15
	A. NOGAPS SUMMARY -----	15
	B. SPECTRAL DECOMPOSITION METHOD -----	17
III.	SPECTRAL VERIFICATION CASE STUDIES -----	19
	A. NOGAPS 2.0 FORECASTS -----	19
	1. Amplitude Errors in Planetary, Long and Medium Wave Features -----	19
	2. Polar Trough Smoothing and Consistent Positive Errors at High Latitudes -----	25
	3. Major Non-Systematic Error -----	28
	B. NOGAPS 2.1 FORECASTS -----	36
	1. Amplitude Errors in Planetary, Long and Medium Wave Features -----	36
	a. Case Study -----	36
	b. Results of Amplitude Error (NOGAPS 2.0 vs. NOGAPS 2.1) -----	40
	2. Polar Trough Smoothing and Consistent Positive Error at High Latitudes -----	43
	a. Case Study -----	43
	b. Results of Positive Error at High Latitudes (NOGAPS 2.0 vs. NOGAPS 2.1) -----	45
	3. Major Non-Systematic Error -----	46
IV.	CONCLUSIONS AND RECOMMENDATIONS -----	48
	APPENDIX A -----	53

LIST OF REFERENCES ----- 91

INITIAL DISTRIBUTION LIST ----- 93

# LIST OF FIGURES

1.	4 November 1983 Analysis of Total Wave Field -----	53
2.	4 November 1983 48-hr Forecast Error of Total Waves -----	54
3.	a) 4 November 1983 48-hr Planetary Wave Forecast and b) Corresponding Analysis for 6 November 1983 -	55
4.	4 November 1983 48-hr Planetary Wave Forecast Error -----	56
5.	a) 4 November 1983 48-hr Long Wave Forecast and b) Corresponding Analysis for 6 November 1983 -	57
6.	4 November 1983 48-hr Long Wave Forecast Error ----	58
7.	a) 4 November 1983 48-hr Medium Wave Forecast and b) Corresponding Analysis for 6 November 1983 -	59
8.	4 November 1983 72-hr Planetary Wave Forecast Error -----	60
9.	a) 4 November 1983 72-hr Planetary Wave Forecast and b) Corresponding Analysis -----	61
10.	4 November 1983 72-hr Long Wave Forecast Error ----	62
11.	a) 4 November 1983 72-hr Long Wave Forecast and b) Corresponding Analysis -----	63
12.	a) 4 November 1983 120-hr Planetary Wave Forecast and b) Corresponding Analysis -----	64
13.	4 November 1983 120-hr Planetary Wave Forecast Error -----	65
14.	a) 4 November 1983 48-hr Total Forecast Error and b) 48-hr Medium Wave Forecast Error -----	66
15.	4 November 1983 48-hr Forecast Error for a) Planetary Waves and b) Long Waves -----	67
16.	4 November 1983 96-hr Forecast Error for a) Planetary Waves and b) Long Waves -----	68
17.	Polar Stereographic Plot of Average Height Field for Month of November 1983 -----	69

18.	Polar Stereographic Plot of 24-hr Average Forecast Error for November 1983 -----	70
19.	Polar Stereographic Plot of 96-hr Average Forecast Error for November 1983 -----	71
20.	a) 4 November 1983 48-hr Total Wave Forecast and b) Corresponding Analysis -----	72
21.	a) 4 November 1983 120-hr Total Wave Forecast and Total Error -----	73
22.	4 November 1983 120-hr Planetary Wave Forecast Error -----	74
23.	Hovmoller Diagram of Total Forecast Error for 4-9 November 1983 -----	75
24.	Hovmoller Forecast Error Diagrams of a) Long Waves and b) Planetary Waves for 4-9 November 1983 -----	76
25.	5 January 1984 Analysis of Total Wave Field -----	77
26.	a) 5 January 1984 72-hr Planetary Wave Forecast and b) Corresponding Analysis for 8 January 1984 --	78
27.	5 January 1984 72-hr Planetary Wave Forecast Error -----	79
28.	a) 5 January 1984 96-hr Medium Wave Forecast and b) Corresponding Analysis -----	80
29.	a) 5 January 1984 120-hr Planetary Wave Forecast and b) Corresponding Analysis -----	81
30.	a) 5 January 1984 120-hr Long Wave Forecast and b) Corresponding Analysis -----	82
31.	5 January 1984 72-hr Forecast Error for a) Total Waves and b) Medium Waves -----	83
32.	5 January 1984 120-hr Forecast Error for Total Waves -----	84
33.	Polar Stereographic Plot of 500mb Average Height Field for December 1983 -----	85
34.	Polar Stereographic Plot of 48-hr Average Forecast Error for December 1983 -----	86

35.	Polar Stereographic Plot of 96-hr Average Forecast Error for December 1983 -----	87
36.	Polar Stereographic Plot of 500mb Average Height Field for January 1984 -----	88
37.	Polar Stereographic Plot of 48-hr Average Forecast Error for January 1984 -----	89
38.	Polar Stereographic Plot of 96-hr Average Forecast Error for January 1984 -----	90

### ACKNOWLEDGEMENT

I want to take this opportunity to express my sincere gratitude to Dr. Carlyle H. Wash for his guidance during the preparation, development and writing of this thesis. His enthusiasm and knowledge of the subject matter are largely responsible for its completion. I would also like to thank my co-advisor Dr. James Boyle for his timely aid and assistance in employing his spectral decomposition software. Without it, I never could have achieved what I set out to do.

Together these gentlemen encouraged and inspired me with their professional dedication and scientific approach in dealing with any problems or questions I brought to them. The major portion of the knowledge which I'll take with me is due in no small part to the give-and-take sessions we shared during the course of my thesis.

Finally, I want to thank my wife, Linda, for her loving support and understanding. Over the last two years (especially the last six months) I haven't been able to spend much time with her and the children. They never complained because they knew I was studying or working on my thesis. Every man should be so fortunate to have such a family. I love them very much.

## I. INTRODUCTION

A major goal for civilian and military atmospheric sciences is accurate and reliable numerical weather prediction. An important aspect of numerical model development is verification studies which can isolate model strengths or weaknesses and indicate errors which must be eliminated to extend the level of forecast skill.

This thesis will investigate the Navy Operational Global Atmospheric Prediction System (NOGAPS) model forecasts of the position and movement of waves at the 500mb level. NOGAPS had been a project of the Naval Environmental Prediction Research Facility (NEPRF) since 1976 and became operational in the fall of 1982 at Fleet Numerical Oceanography Center (FNOC). The long term goal of NOGAPS is to achieve a medium range (7-10 days) numerical forecast capability for the United States Navy (Rosmond, 1981).

An integral part of this effort is verification of NOGAPS. As the NOGAPS model is a modified form of the UCLA general circulation model, it does not have the benefit of many intensive verification studies as have most second and third generation operational models.

Recent studies have raised serious questions concerning the relative accuracy of the planetary-scale (zonal wavenumbers 1-2) wave motion forecasts of the 500mb level produced by numerical weather prediction models. Miyakoda et al.

(1972) examined the GFDL model for a series of winter forecasts and found that the planetary-scale motion predictions of a spectral numerical model were poorer with respect to persistence than the predictions of long (wavenumbers 3-5) or medium-scale (wavenumbers 6-10) motions. Lambert and Merilees (1978) found similar error characteristics in their planetary-scale forecasts. Somerville (1980) examined the planetary-scale wave forecasts of a primitive equation numerical model in both a hemispheric and global configuration. He concluded that the global version had substantially more skill than the hemispheric version; particularly so in the latter portion of the five-day forecast period. Bettge (1981) in a study of planetary-scale forecast errors of the NMC operational, primitive equation, grid-point model noted that oscillations in the total 72-hr forecast error time series were closely correlated to those in the planetary scales.

This study will verify NOGAPS planetary wave forecasts and other wave regimes, large and medium-scale. Both forecast and analysis data from 500mb are spectrally decomposed into their basic components of amplitude and phase, then grouped into planetary, long and medium-scale waves for individual analysis of their atmospheric characteristics.

Errors in amplitude, phase speeds, baroclinic system development and dampening of planetary wave structure and smaller scale features become readily apparent when the

forecasted variables are analyzed over time via a Hovmoller or trough-ridge plot. This technique was utilized by Baumhefner and Downey (1978) to compare the forecasting skills of three different numerical weather prediction models. Somerville (1980) also utilized this method to examine planetary-scale wave forecasts of a primitive equation numerical model in both global and hemispheric configurations. Forecasts which originally appeared quite good were analyzed only to have amplification errors emerge in many of the transient systems.

In this study the Hovmoller plot is broken down spectrally into planetary (wavenumbers 1-3), large (wavenumbers 4-7), and medium-scale (wavenumbers 8-12) waves. Capt. Morse (1983) conducted a spectral verification of NOGAPS 500mb forecasts for one three-day and two five-day cases. By analyzing the trough-ridge (Hovmoller) diagrams of longitude versus time for each wave group, he noted that in all three cases the most serious errors occurred in the planetary waves where the model forecast erroneously large or small amplitudes. Most accurately forecast were the long waves while the medium wave amplitudes were under-forecast and the phase speeds were too fast.

The specific objectives of this thesis are to:

- (1) Employ existing spectral verification software developed by Dr. James Boyle using wavenumber grouping and Hovmoller plots to analyze interesting NOGAPS 00-120 hour

forecast situations at 500mb and expand the analysis of Morse (1983).

(2) Analyze 5-day forecasts from both NOGAPS 2.0 and NOGAPS 2.1 models to ascertain if the major model modification of adding three additional vertical layers improves forecast performance.

(3) Use wavenumber analysis with Morse's results to isolate systematic errors in planetary, long and medium-scale waves.

Chapter II gives a brief summary of the NOGAPS model and an illustration of the spectral decomposition method application. Chapter III presents case studies of both NOGAPS 2.0 (six-layer) and NOGAPS 2.1 (nine-layer) models which identify forecast deficiencies present in the majority of the cases for each model version. The two model versions will be compared to determine improvement of characteristic or systematic error. In Chapter IV, conclusions of applying spectral analysis and utilizing Hovmoller diagrams to analyze NOGAPS forecasts are presented. Recommendations for further research in this area follow.

## II. NOGAPS SUMMARY AND SPECTRAL VERIFICATION APPROACH

### A. NOGAPS SUMMARY

The Navy Operational Global Atmospheric Prediction System (NOGAPS) model is a modified version of the UCLA general circulation model (GCM). The following section describes the various features of NOGAPS. The complete model has been described by Rosmond (1981).

The dynamics of the UCLA GCM are described in detail by Arakawa and Lamb (1977). NOGAPS is a primitive equation model utilizing horizontal velocity,  $U$  and  $V$ , temperature,  $T$ , surface pressure,  $P$ , and specific humidity,  $q$ , as prognostic variables. The horizontal grid has a spatial resolution of 2.4 degrees latitude by 3.0 degrees longitude with the variables staggered according to Arakawa scheme C. The center grid point contains the mass variables ( $T$ ,  $P$ , and  $q$ ). The meridional wind component,  $V$ , is carried at points north and south of the center point and the zonal wind component,  $U$ , is carried at points east and west of the center point. The numerical differencing scheme is both energy and enstrophy conserving when the flow is nondivergent.

NOGAPS uses a sigma vertical coordinate system. Until December 1983 there were six model vertical layers. With the upgrade of the model an additional 3 layers (plus other minor model modifications) have been included and are

arranged to give increased vertical resolution in the lower tropospheric region with the top of the model atmosphere at 50mb. All prognostic variables are carried at the middle of each layer except vertical velocity which is carried at the layer interfaces.

NOGAPS employs filtering techniques to maintain computational stability at high latitudes and aid in the assimilation of diabatic effects. In the high latitude area the zonal grid interval becomes too small to allow the model to remain computationally stable for the time step used. A hybrid filtering scheme is used. For latitude rings poleward of 60 degrees, a special Fourier filtering procedure is used. Equatorward of these Fourier filtering areas, a very fast three point filter is used which is not scale selective, but is computationally efficient. This filtering smoothes the amplitude of the zonal mass flux and zonal pressure gradients with a longitudinal averaging operator. A more detailed explanation of this filtering technique is provided by Arakawa and Lamb (1977).

The planetary boundary layer (PBL) is defined as a well mixed layer in moisture, momentum and moist static energy. The PBL treatment follows Deardoff (1972) and allows for interaction between the PBL and cumulus cloud ensembles at each grid point. A special feature of the model is the variable depth of the PBL in the lowest layer which is capped with a "porous" material surface to allow entrained

mass to deepen the PBL and remove mass by cumulus mass flux to decrease the PBL. Cumulus parameterization in NOGAPS follows the scheme of Arakawa-Schubert (1974) as described by Lord (1978). The radiation parameterization follows Katayama (1971) and Schlesinger (1976) and uses bulk transmission functions for discrete pressure layers. Net radiative flux at ground level is a function of incoming solar and longwave radiation and surface albedo.

#### B. SPECTRAL DECOMPOSITION METHOD

The verification approach uses spectral analysis by which a periodic function can be broken down into its harmonic components. Any arbitrary function (a waveform) can be represented by a Fourier series. In our application, a Fourier decomposition is applied to the 500mb height field. By summing over all wavenumbers the wave pattern is transformed back into its original shape. The equation utilized in the algorithm is of the form:

$$\phi_{\lambda} = \sum n A_n \sin n(\lambda) \quad (1)$$

where  $n$  is the respective wave number and  $\lambda$  is a function of longitude.

Morse (1983) and others have shown that the complex appearance of a typical 500mb height wave pattern can conceal the sources of forecast error. The pattern complexity is due to the superposition of planetary, long, medium and

synoptic scale waves. To aid in the forecast verification, wavenumber groupings (forecast vs. observed) are analyzed rather than just the total field. The spectral decomposition of the 500mb wave pattern is analyzed by zonal wavenumber component and then grouped into planetary (wavenumber 1-3), long (wavenumber 4-7) and medium (wavenumber 8-12) waves. The spectral analysis used in this study was developed at the Naval Postgraduate School by Dr. James Boyle.

This approach permits an analysis of the accuracy of the forecast for the various scales of motion. Employing this technique, one can readily ascertain if the errors in the total field are attributable to errors in certain wave lengths. Further clarification is provided by the analysis of the error (forecast minus analysis) for each of these wave number groups.

### III. SPECTRAL VERIFICATION CASE STUDIES

In this chapter the spectral decomposition method presented previously is employed to verify several NOGAPS 2.0 120-hr forecasts from the spring and winter of 1983. Then, in the following section, it is utilized to analyze several NOGAPS 2.1 120-hr forecasts from the winter of 1983-1984 for comparative purposes. For both models (NOGAPS 2.0 and NOGAPS 2.1) the 5-day forecast periods available for study are low-index situations with dominant planetary (WN 1-3) and long wave (WN 4-7) activity. All forecasts are from 0000 GMT and are verified at 24, 48, 72, 96 and 120 hours of the forecast period.

#### A. NOGAPS 2.0 FORECASTS

Four 120-hr forecasts were obtained for the six-level model version. They were for 11-16 April 1983, 04-09, 14-19, and 24-29 November 1983 periods. It is the intent of this study to identify errors which are representative of those found in the majority of the 5-day forecasts.

##### 1. Amplitude Errors in Planetary, Long and Medium Wave Features

The first type of error noted in the NOGAPS 2.0 forecasts was the lack of amplitude or smoothing of the height field in troughs and ridges at the 500mb level. This pattern of error was noted in all four NOGAPS 2.0

forecasts. The 11-16 April 1983 forecast, however, did not demonstrate it as consistently as the other three forecasts. The 5-day forecast for the 04-09 November 1983 timeframe is most representative of those three cases. The upper-level flow at the beginning of the forecast period is shown in Figure 1. Of note is the three large (planetary-scale) ridges over Asia, North America, and Europe. In the Southern Hemisphere, the long waves dominate the flow.

By 48 hours into the forecast several areas of the globe display errors due to lack of amplitude. Over Asia the ridge is underforecast (heights too low) as seen by the negative error of 120m in the total wave error plot (Fig. 2). A plus error indicates the model has forecast the height contours too high and a negative error the heights are too low. Over Europe a negative error of 180 m is noted. In the Southern Hemisphere east of the Falkland Islands (60S, 20W) 180 m of negative error is observed. Some insight as to the source of this error can be gained by examining the various wavenumber groups. Figures 3a and 3b are the planetary wave (WN 1-3) 48-hr forecast and corresponding analysis. A cursory comparison between the forecast and the analysis seems to indicate the model has made an adequate forecast. The planetary wave 48-hr forecast error plot (Fig. 4), however, reveals error patterns associated with the lack of amplitude. The negative error over Asia (60 m) and over Europe (100 m) indicates the ridges have been smoothed in

these regions. In the Southern Hemisphere, an area of negative error (90 m) is noted east of the Falkland Islands. Again, this is due to the ridging being flattened out or smoothing of the height field in the forecast (Fig. 3a vs. 3b).

Looking at the long waves (WN 4-7), further evidence of the model smoothing out the upper-level features is noted. The 48-hr long wave forecast and corresponding analysis are represented in Figures 5a and 5b. The model has depicted a ridge over eastern Asia centered at 120 E. The analysis shows the ridge to be more intense and further west than forecast. The model also has not reflected the shallow trough which has formed at 130 E. The 48-hr forecast error plot for the long waves (Fig. 6) indicates smoothing of the ridge over Asia by the negative error (90 m) and the missed trough by the positive error of 60 m.

In the analysis (Fig. 5b), there is a series of long waves which start with the ridge south of Alaska and undulate eastward to the ridging over the Maritime Provinces. The model (Fig. 5a) readily shows smoothing of these ridges and troughs in this series of waves. This is confirmed by the error plot (Fig. 6) which discloses the negative error (60-90 m) for the flattened ridges south of Alaska and over the Maritime Provinces. The troughs over the eastern Pacific Ocean and over the New England states (Fig. 5b) were under-forecast (heights too high) by the model (Fig. 5a). This

resulted in the positive errors noted over those areas in the long wave 48-hr forecast error plot (Fig. 6).

This lack of amplitude is also seen in the shorter wavelengths. Figures 7a and 7b are the 48-hr forecast and corresponding analysis for the medium waves (WN 8-12). When comparing the forecast to the analysis for the region over the United States and eastward, the smoothing is apparent even for these shorter waves.

At 72 hours into the forecast the error due to the lack of amplitude attains a maximum. Figure 8 is the 72-hr error plot for the planetary waves. Note the negative error over Asia (90 m), western Canada (90 m), and over northern Europe (200 m). These areas of negative error correspond to the lack of amplitude in the ridges in the planetary wave forecast (Fig. 9a) versus the analysis (Fig. 9b). Similarly the trough south of the Bering Sea and the trough which extends from Baffin Bay southeast into the Atlantic Ocean are not handled adequately by the model (Fig. 9a vs. 9b). The positive error (Fig. 8) centered over the Kamchatka peninsula (90 m) and over Quebec (120 m) extending to the southeast is indicative of the smoothing of the troughs.

In the Southern Hemisphere an almost classic example of negative errors associated with underforecast ridging and positive errors with underforecast troughing is noted in the planetary waves at 72 hours. Figures 9a and 9b are the planetary wave 72-hr forecast and corresponding analysis.

The error plot for these waves (Fig. 8) corroborates this fact by the presence of positive errors in the vicinity of the troughs (south of New Zealand and the tip of South America). Likewise, negative errors are observed in the error plot that are associated with the ridges at 65 S, 130 W and at 60 S, 10 W. The magnitude of error in Figure 8 varies from plus or minus 60 to 120 m for these smoothed wave features.

For the long waves (WN 4-7), the 72-hr error plot (Fig. 10) in the Northern Hemisphere reveals that the error pattern is similar to that of 24 hours earlier (Fig. 6) except it has propagated eastward and increased in magnitude. Figures 11a and 11b are the 72-hr medium wave forecast and the analysis for 07 November. The underforecast ridge south of Alaska is indicated by the negative error (60 m) in the error plot (Fig. 10). In the error plot the lack of adequate troughing over New England is seen by the plus error (90 m) and the poorly forecast ridging over the Maritime Provinces by the negative error of 150 m.

The model has made a minimal attempt to forecast the large trough over the eastern Atlantic Ocean (Fig. 11a vs. 11b). This is reflected in the error plot (Fig. 10) by a positive error of 120 m. The absence of the ridge over western Europe results in a negative error of 240 m centered over Norway. Although to a lesser degree, the model exhibits the same tendency in the Southern Hemisphere for this wave

group regime. Like that of the long waves, the medium wave (WN 8-12) error increases in magnitude and the pattern shifts as the features propagate eastward.

Throughout the remainder of the forecast period, the model performance is degraded further in most regions of the globe. Most notable is the planetary wave forecast at 120 hours. Figure 12a is the planetary wave 120-hr forecast and Figure 12b the corresponding analysis. The blocking ridge over western North America is poorly forecast by the model. The large trough which extends from Quebec southeast into the eastern Atlantic Ocean is ignored by the model and results in a positive error of nearly 200 m in the planetary wave 120-hr forecast error plot (Fig. 13).

Most noteworthy of this error pattern is the extremely large magnitude of error (minus 360 m) noted over Europe in Figure 13. This large error is a direct result of the model inability to accurately forecast the extensive planetary-scale ridging which occurred over Europe (Fig. 12a vs. 12b). The other three forecasts 14-19 and 24-29 November and 11-16 April did not demonstrate amplitude errors of this magnitude. Errors ranged from 120-180 m for the planetary waves, 100-140 m for the long waves and 40-90 m for the medium waves.

This general pattern of error (negative with ridges and plus with troughs) was noted in all of the 5-day forecasts for the NOGAPS 2.0 version. The magnitudes of these amplitude errors will be discussed in a later section when

compared to that of NOGAPS 2.1. Although the resultant error in this example was the largest observed, this case demonstrated the errors noted in the other three forecasts.

2. Polar Trough Smoothing and Consistent Positive Errors at High Latitudes

The second pattern of error noted in the NOGAPS 2.0 model forecasts is the extensive amount of positive error located at high latitudes (poleward of 70 degrees). This error pattern was readily apparent in three of the four 5-day forecasts examined. The 04-09 November 1983 case was the exception where negative error appeared in the Southern Hemisphere and persisted throughout the forecast.

Most illustrative of this error pattern is the 5-day forecast for 14-19 November 1983. Figure 14a is the 48-hr error plot for the 500mb total wave field. In the Northern Hemisphere regions of positive error at high latitude are noted north of Asia, North America, Greenland and Europe. In the Southern Hemisphere, positive error is observed almost everywhere poleward of the Antarctic coastline. Figure 14b is the 48-hr error plot for the medium waves (WN 8-12), the smallest wave group examined. Note the almost zonal nature of the positive error pattern (from 30-90 m) poleward of 70 degrees in the Northern Hemisphere. In the Southern Hemisphere the positive error pattern is also consistently widespread but of less magnitude.

Figures 15a and 15b are the 48-hr error plots for the planetary and long waves at 500mb. Positive error is

noted around the globe near both poles in the planetary wave error plot (Fig. 15a) attaining 90 m in the Northern Hemisphere. The 48-hr error plot for the long waves (Fig. 15b) reveals a consistent positive error (60-90 m) around the Arctic. The error around Antarctica is also positive but somewhat irregular in shape due to the amplitude smoothing of the long wave features and resultant plus-minus-plus error pattern. This plus-minus-plus error pattern (Fig. 15b) tends to disrupt the pattern of positive error growth near the poles.

By 96 hours into the forecast the magnitude of positive error has increased substantially in both hemispheres. The pattern of error has been maintained from 48 hours earlier while the magnitude has doubled throughout most of the various wavenumber groupings. This can readily be seen by comparing the 96-hr forecast error plots of each wavenumber grouping to that of 48 hours. For the planetary waves, comparing Figure 16a to 15a reveals the twofold increase in the magnitude of positive error for the Northern Hemisphere high latitude region. In the Southern Hemisphere the magnitude has also increased but unlike the Northern Hemisphere the pattern is dissimilar to that of 48 hours earlier.

For the long waves (Fig. 16b vs. 15b), the pattern similarity and twofold increase in error magnitude is replicated in the Northern Hemisphere. In the Southern Hemisphere the error magnitude is doubled while the pattern is only

similar to that of 48 hours. For the medium waves the pattern is quite similar and the increase in magnitude is again twofold to that of 48 hours earlier in both hemispheres.

Although the previous figures readily show the consistent positive error present near the poles, being Mercator projections they flatten the curvature of the features at high latitudes. Figure 17 is a polar stereographic projection of the 500mb height field for the Northern Hemisphere. This figure shows the monthly average of the daily analyses of the 500mb level for November 1983. For the purpose of graph orientation, the meridians for every 30 degrees are shown. The Greenwich Meridian is at the eleven o'clock position, the west coast of the United States at three o'clock and the islands of Japan just west of six o'clock. Note the prominent troughs over the Aleutian Islands and over Baffin Island.

Figure 18 is the monthly average of the 24-hr forecast errors for November 1983. The heavy dark line is the zero line which encompasses the region of positive error near the North Pole. Note also the extension of the positive error equatorward where the polar troughs were positioned in the plot of the 500mb height field (Fig. 17). The positive error extending southward in these regions is indicative of the smoothing of the polar troughs. Figure 19 is the monthly average error for November 1983 for the 96-hr forecasts. The magnitude of the average error for 96-hr

forecast has increased to 90 m with an extension southward over Baffin Island. The use of these monthly average error plots highlights the consistent positive error near the poles and illustrates the amplitude smoothing of the polar troughs.

### 3. Major Non-Systematic Error

This section presents an error which was not observed in the majority of the NOGAPS 2.0 forecasts but was noteworthy nonetheless. In two forecasts for the month of November the model was unable to forecast the development and intensification of a cutoff low over eastern North America. The error not only increases with time but appears to spread into the larger waves with disastrous results. This case highlights the growth of larger scale error in response to smaller scale forecast error upstream.

The NOGAPS 2.0 model version encountered difficulty in forecasting the 500mb height flow downstream of the east coast of North America. Looking at the flow over the North American continent and eastward, NOGAPS exhibits a tendency for underdeveloping intensifying long wave troughs by 48 hours into the forecast. Instead of the trough deepening and subsequent development into a cutoff low, the trough is slowly filled and is displaced too far east and northward. The net effect is "smoothing" of the wave curvature of the troughs and ridges downstream. This diminished wave amplitude is propagated throughout the forecast period so that by 120 hours the forecast is of little value or the flow

misrepresents the meridional nature of the upper-air flow pattern over a region of 50-100 degrees of longitude.

This error was vividly demonstrated in the model 5-day 500mb forecast for the 04-09 November 1983 timeframe. The 500mb wave pattern (Fig. 1) at the onset of the forecast period indicated the dominance of Planetary-scale (WN 3) flow with ridging over Asia, North America and Europe. Of particular interest for this discussion is the nearly cutoff low which has formed over the Great Lakes region and the ability of the model to depict its development throughout the forecast.

By 48 hours, the model starts filling the low over the eastern United States instead of maintaining it as a cutoff low as observed on 06 November (Figs. 20a and 20b). The trough downstream (which has deepened into a long-wave trough over the Atlantic Ocean) has been totally missed by the model. Further downstream the ridging into western Europe is absent.

The magnitude of these errors at 48 hours is clearly seen in the difference plot (Fig. 2). The missed cutoff low over the eastern United States is reflected by a positive error (heights too high) of 120 m. The missed long-wave trough over the Atlantic Ocean results in a positive error of 240 m. Further east the negative error noted over the United Kingdom reflects the inadequate ridging into western Europe.

Investigating the source of these errors is facilitated by examining the 48-hr difference plots for the planetary (WN 1-3) and long (WN 4-7) waves. Over the eastern United States, the planetary-wave errors (Fig. 4) are minimal but increase in magnitude across the Atlantic Ocean where they are positive then become negative approaching western Europe. Looking at the planetary-wave forecast and corresponding analysis (Figs. 3a and 3b) helps explain the errors noted on the difference plot (Fig. 4). The ridge over North America lacks adequate NW-SE tilt, in addition, the forecasted ridge is approximately 20 degrees out of phase as it is displaced too far east. The negative errors over Europe (Fig. 4) are a result of the lack of amplitude in the ridge due to smoothing of the height field (Fig. 3a vs. 3b).

Looking at the long wave errors in Figure 6, a different error pattern is noted. Commensurate with the scale of the missed cutoff low and the long-wave trough mentioned earlier, a plus-minus-plus-minus pattern (of equal magnitude of plus or minus 90 m) emerges immediately over the eastern United States and extends into Europe.

Comparing the long-wave forecast and corresponding analysis (Figs. 5a and 5b) reveals the nature of these errors. From the eastern side of the North American continent eastward over into Europe, the meridional nature of the observed flow (Fig. 5b) is poorly represented in the forecast (Fig. 5a). The trough over the New England states and

ridging up over the Maritime Provinces is smoothed out. The long-wave trough over the middle of the north Atlantic Ocean is virtually non-existent and the subsequent downstream meridional flow over into Europe is so poorly forecast that an entire wave appears to have been omitted. From 80 degrees W to 40 degrees E only two waves seem to be forecast when in fact three distinct waves are observed.

By 72 hours the difference plot (not shown) reveals the plus-minus-plus pattern of error has been maintained but shifted slightly eastward. The magnitude of this plus and minus error has increased significantly over the Atlantic Ocean and Europe respectively. This reflects the inability of the model to capture the intensifying trough and extensive ridging over these regions. The net result is the model has dampened the 500mb features to the extent that the flow is erroneously depicted as zonal by 72 hours.

The magnitude of the planetary wave error over Europe is minus 180 m. The negative error over Europe for the long waves is quite extensive (240 m) illustrating the dampening of these waves. This large error appears to be the result of two factors:

- (1) The 500mb flow from the United States to Europe is dominated by long wave features during this portion of the forecast, and
- (2) The low-index features of the long waves are totally misrepresented in the forecast as nearly zonal flow is

depicted. This is not just a case of the model "smoothing out" the amplitude of existing wave features. It reflects the inability of the model to develop these features.

The observed flow at 500mb has become more meridional by 96 hours. The model makes a belated (albeit feeble) attempt to depict the ridging east of the Maritime Provinces and the large trough over the Atlantic Ocean. The huge blocking high over Europe is virtually absent. The difference plot (not shown) reflects this by the large negative error (420 m) over Europe. By this time the planetary wave error (minus 300 m) comprises the bulk of the total error.

By 120 hours into the forecast the model begins to reflect the low-index flow (Fig. 21a) over North America and the Atlantic Ocean of 36 hours earlier. The forecast has still neglected to depict, however, the extensive ridging that has occurred over Europe. As was noted at 96 hours, the extensive region of negative error over Europe (Fig. 21b) is still present. The large trough over the eastern Atlantic Ocean has developed into a large cutoff low which the model has depicted as a moderate trough (Fig. 21a). This accounts for the plus 240 m error over this region in Figure 21b.

The extensive negative error noted over northern Europe which extends into Greenland (Fig. 21b) has been shown to be related to that (error) of the planetary-scale wave forecast. Nowhere is this more evident than when comparing the planetary wave error at 120 hours (Fig. 22) with the

error of the total 500mb surface (Fig. 21b). Note the similarity in the position, shape and magnitude of the two regions of error.

An examination of the analysis of the planetary waves for 09 November (Fig. 12b) reveals the extent of ridging which has taken place over Europe. Also noteworthy is the pronounced NW-SE tilt of the ridge. The corresponding 120-hr forecast (Fig. 12a) of the planetary waves is unique in two ways:

- (1) It has completely ignored the development of this substantial ridge (and the trough over the Atlantic Ocean), and

- (2) It has maintained this same high-index flow regime throughout the forecast with little if any change.

By utilizing Hovmoller (longitude-time) plots, information can be obtained to aid in summarizing the problems encountered by the model. The plots for this particular case are fixed at 50 N latitude. This latitude was chosen as being optimal in reflecting the majority of features discussed. The plots are made by first computing a zonal average (of the height values) over a ten-degree latitude band around the globe. Ten degrees was selected as very little difference was noted from larger or smaller values. Also, it was felt to be most representative in that it would best depict the features of the scales in this study. This band is centered on whatever latitude is chosen.

The values which label the contours represent the height above or below the zonal average. In addition, plots for the total height field, plots for each wave-number grouping are also utilized. This breakdown should aid the verification process by graphically depicting the evolution of error for each wave number group. In this manner, some insight can be gained as to the source of the error.

Figure 23 is the Hovmoller difference plot for the 500mb total field. Our main region of interest in this case is from 80 W and eastward. Keep in mind the height field is averaged over ten degrees of latitude so the magnitude of the errors has been reduced. At approximately the 24-hr mark, the missed long-wave trough which formed and intensified over the Atlantic Ocean is noted by the positive error at 30 W. The error increases and moves slowly eastward during the forecast period. At 60 W the negative error from the poorly forecast ridging over the Maritime Provinces is noted by 36 hours. The inability of the model to forecast the extensive ridging over Europe is noted by the negative error appearing relatively early in the forecast and increasing rapidly after 48 hours.

Examining the Hovmoller difference plot for the long waves (Fig. 24a) reveals the difficulty the model has in accurately depicting these waves early on in the forecast period. The error in the planetary waves (Fig. 24b) appears approximately 24 hours later and increases with time. In

this case, the inability of the model to develop the cutoff low over the eastern United States had a major impact on the forecast success downstream. The Hovmoller plots seem to indicate the error was then propagated into larger wave regimes during the first 48 hours of the forecast period which manifested into substantial errors in the planetary waves later in the forecast.

In addition to the poor forecast of the cutoff low over the eastern United States, there was another synoptic-scale feature which contributed to the planetary-scale error noted in this forecast. The model also poorly handled a case of maritime cyclogenesis over the middle of the Atlantic Ocean. A review of surface analyses for the 04-09 November 1983 timeframe revealed a low-pressure system which deepened very rapidly during the early portion of the forecast period. Early on in the forecast the model adequately depicted the decreasing pressure at the surface level. By 36 hours, however, the model began diminishing the rate of pressure decrease and moving the system too fast. As a result the low-pressure system was displaced to the northeast ahead of its actual position and under-intensified. It is difficult to determine if this low-pressure system at the surface was poorly forecast due to the lack of model upper-air support. Likewise, it could have developed in the lower troposphere and contributed to the 500mb level model error downstream over Europe.

NOGAPS 2.0 also experienced similar difficulty in predicting the development and movement of long wave features over eastern North America in just one other forecast. This planetary wave error growth in response to shorter wave error upstream also occurred in the 5-day forecast for 24-29 November 1983. The error in the 24-29 November forecast did not approach the magnitude of that seen in the 4-9 November period. As this error pattern was not demonstrated in the majority of the NOGAPS 2.0 forecasts nor off the east coast of Asia, it was not felt to be systematic in nature.

#### B. NOGAPS 2.1 FORECASTS

Eight 120-hr forecasts were obtained for the NOGAPS 2.1 (nine-level) model for verification purposes. These were for 9-14, 21-26 and 26-31 December 1983. For the month of January 1984 forecasts were 1-6, 5-10, 11-16, 21-26 and 26-30 timeframes.

##### 1. Amplitude Errors in Planetary, Long and Medium Wave Features

This pattern of error was observed in four of the 5-day forecasts for the NOGAPS 2.1 model version. They were the 21-26 and 26-31 December 1983 and the 5-10 and 15-20 January 1984 forecasts.

##### a. Case Study

The 5-day forecast for 5-10 January 1984 best illustrates this error pattern for the NOGAPS 2.1 forecasts. Figure 25 is the 500mb analysis for 5 January which depicts

the flow at the beginning of the forecast period. The Northern Hemisphere is dominated by planetary-scale features with a large ridge located over central Asia. A large trough is positioned over the western two-thirds of the north Pacific Ocean. Moderate ridging is noted over western North America while troughing occurs over the eastern portion of the continent. In the Southern Hemisphere long waves dictate the pattern of flow from Australia eastward to South America.

By 72 hours into the forecast amplitude smoothing is noticed in the planetary and long wave features. Figures 26a and 26b are the 5 January 72-hr forecast and corresponding analysis for the planetary waves. The large trough located over the Kamchatka peninsula is underforecast by the model. The ridging over western North America which extends up over Alaska is also underforecast. The shallow trough over eastern North America associated with the low centered over Baffin Island lacks amplitude. Continuing eastward the ridging over the Atlantic Ocean appears to be dampened.

This smoothing is verified by examining the 72-hr error plot (Fig. 27) for the planetary waves. The underforecast trough over Kamchatka is noted by the plus 60 meters error. The inadequate ridging over Alaska is seen by the negative error of 180 meters. The shallow trough over eastern North America shows minimal dampening (less than 60 meters) while the ridging over the Atlantic Ocean has been underforecast

by 120 meters. Although not shown, the long waves at 72 hours were only appreciably dampened in the Southern Hemisphere. Features in the Northern Hemisphere were depicted adequately except the ridge over the Atlantic Ocean which was underforecast. The medium waves displayed minimal dampening but began to experience phase errors.

By 96 hours the error pattern of the planetary waves (not shown) is quite similar to that of 24 hours earlier. The only departure is the increased negative error over the Atlantic Ocean as the building ridge is underforecast. The long waves (also not shown) in the Northern Hemisphere experience moderate dampening during this period. In the Southern Hemisphere the model is more successful as dampening of the long wave features is minimal. The medium waves readily demonstrate amplitude dampening in the Northern Hemisphere from 160 E to 90 W (Figs. 28a vs. 28b).

By the end of the forecast period (120 hours) amplitude smoothing appears in all wave groupings. Figure 29a and 29b are the 120-hr forecast and corresponding analysis of the planetary waves. Although the error plot is not shown, the dampening of these features is readily noted. The trough over the Kamchatka peninsula is underforecast by 100 m while the extensive ridging up over Alaska is dampened by 240 m. The lack of troughing over the eastern portion of North America results in a positive error of 180 m. The ridging in Europe is underforecast by 180 m.

The long wave forecast and corresponding analysis at 120 hours (Figs. 30a vs. 30b) also demonstrate amplitude smoothing. Those features significantly dampened are the ridge over western North America (minus 120 m error) and the trough over Europe (plus 180 m error). The lack of ridging into Asia (30E-60E) resulted in a minus error of 120 m. The error plot for the long waves is not shown. The medium waves (not shown) experience mostly phase error by this time in the forecast period.

Although this error pattern was noted in three other forecasts, none demonstrated this error consistently in all wave groupings throughout the 5-day period. One of these forecasts (15-20 January) which displayed amplitude smoothing simultaneously exhibited amplitude intensification in the planetary waves. This planetary wave event occurred in the Northern Hemisphere while the expected pattern of error (smoothing) was noted in the Southern Hemisphere.

At 48 hours into the forecast a large cutoff low was centered over the islands of Japan. Adjacent to the low a large blocking high was located which extended poleward to 80 N. The model had over-intensified the low (too deep) by 100 m. The high (depicted only as a ridge in the forecast) was underforecast by the model by approximately the same amount. By 96 hours the forecast cutoff low was still too deep but the model had begun to over-develop the blocking ridge. By 120 hours the model had over-developed both the

low (too deep) and the ridge (too high). Although both model versions would occasionally over-intensify a wave feature, this event was unique because the model initially underforecast it. This was not observed in any of the other forecasts.

b. Results of Amplitude Error (NOGAPS 2.0 vs. 2.1)

The NOGAPS 2.0 forecasts generally demonstrated sufficient smoothing of the 500mb height contours to register sizeable errors by 48 hours. Smoothing of trough and ridge features resulted in errors ranging from 60-90 m for the planetary waves. For the long waves three of the four forecasts experienced minimal dampening (30 m error). The exception to this was the 4-9 November forecast which exhibited a very large error (90-120 m) due to excessive smoothing over eastern North America into the Atlantic Ocean. The medium waves were dampened 30-60 m but the error was restricted to approximately 80-120 degrees of longitude.

The NOGAPS 2.1 forecasts by 48 hours were more successful. In predicting the amplitude of the planetary waves, errors ranged from 40-60 m compared to 60-90 m for the older model version. The long wave forecasts did not improve on those of the older model version. Long wave forecast error (30-40 m) due amplitude smoothing was similar to that of the 2.0 version. The medium wave forecast at 48 hours enjoyed moderate forecast success reducing the error by 10-20 m. Overall, two of the three wave groups in NOGAPS

2.1, planetary and medium, demonstrated less forecast error compared to NOGAPS 2.0.

By 72 hours NOGAPS 2.1 displayed some degree of forecast improvement in all wave groups compared to NOGAPS 2.0. The dampening of the planetary waves resulted in errors of 60-100 m compared to 75-120 m for NOGAPS 2.0. Long wave forecasts for NOGAPS 2.1 exhibited smoothing errors of 60-90 m versus 60-120 m for the older model version. NOGAPS 2.1 medium wave forecast error was 30-60 m compared to 50-70 m for NOGAPS 2.0. Several of the medium wave forecasts in both model versions experienced phase error (too fast) by this time in the forecast period. This complicated the determination of smoothing error.

At 96 hours the forecast error due to amplitude smoothing attains a maximum in both model versions. Dampening of the planetary waves in NOGAPS 2.1 was reflected by the 60-160 m range of error compared to 80-180 m for the older model version. NOGAPS 2.1 long wave forecast errors were from 70-130 m while those of NOGAPS 2.0 ranged from 85-140 m. As was noted 24 hours earlier, the long wave forecast error is only slightly less than that of the planetary waves. Only modest forecast improvement is evident in the newer model version for the long waves. Both model versions exhibit approximately the same amount of dampening error (50-60 m) for the medium waves at 96 hours. Some phase error remains but appears to have decreased in the newer model version.

At 120 hours the error attributable to amplitude smoothing generally did not increase from that of 24 hours earlier. Any increase in error was usually a result of phase difference and insufficient or incorrect axis tilt. As far as could be determined, NOGAPS 2.1 was much more successful than NOGAPS 2.0 in correctly forecasting the tilt of the wave axis.

After a quantitative comparison of the two model versions, NOGAPS 2.1 demonstrated limited success over NOGAPS 2.0 with respect to amplitude smoothing and resultant error magnitudes. From the 48 hour mark to the end of the period reductions in forecast error were only of the order of 10-15 percent.

This study also revealed that the long waves contributed a disproportionately large amount of error to the total forecast error. This was noted for both model versions. This is contrary to the findings of Morse (1983) who found that NOGAPS 2.0 most accurately forecasted the long waves. Part of the explanation for this difference could be that he was only able to examine three cases, one of which only went out to 72 hours and utilized a coarser grid scheme. The newer model version also showed little phase error improvement from that noted for NOGAPS 2.0.

As was mentioned before, when phase errors begin to appear the determination of error due to amplitude smoothing became difficult. Another problem was differentiating

error due to insufficient axis tilt from that of amplitude smoothing. Measures were taken to reflect only that error due to amplitude smoothing. Wave features which exhibited axis tilt of 30 degrees or more (or tilt in the wrong direction) were not used for comparative purposes. Wave features which displayed detectable phase errors were also not used. By employing these criteria for wave feature comparison, the error from sources other than amplitude smoothing would be minimized. Invariably some "contamination error" from extraneous sources will be present. However, those values of comparative error above due to smoothing are felt to be representative.

2. Polar Trough Smoothing and Consistent Positive Error at High Latitudes

This error pattern was noted in all the 5-day forecasts of the NOGAPS 2.1 model version. Four of the forecasts exhibited this error in both hemispheres; two from the month of December 1983 (21-26 and 26-31), and two from January 1984 (5-10 and 26-31). The remaining cases displayed this error in only one hemisphere.

a. Case Study

The forecast for 5-10 January 1984 is representative of the positive error found near the poles for the NOGAPS 2.1 cases. Figure 31a is the 72-hr error plot for the 500mb total wave field. In the Southern Hemisphere the positive error is widespread and attains magnitudes up to 120 m over the Antarctic continent. In the Northern

Hemisphere the error pattern is somewhat irregular and the magnitude of error less (than that of the Southern Hemisphere). Figure 31b is the 72-hr error plot for the medium waves (WN 8-12). Like the NOGAPS 2.0 model version, these smaller waves demonstrate the symmetric latitudinal distribution of error near the poles (Fig. 31b vs. 14b).

By 120 hours into the forecast the error pattern has become widespread throughout both hemispheres. In the 500mb total wave error plot (Fig. 32) note the consistent positive error across the globe at high latitudes. The positive error pattern attains magnitudes of 120 m in the Northern Hemisphere with values slightly lower in the Southern Hemisphere. This is demonstrated in all the wavenumber groupings, planetary, long and medium waves by 120 hours.

Polar stereographic plots of the Northern Hemisphere 500mb height field reveal the positive error and amplitude smoothing of the polar troughs more readily at high latitudes. Figure 33 is the monthly average of the analyses of the 500mb height field for each day of December 1983. The average for December 1983 was computed from the eighth when the NOGAPS 2.1 model version became operational. Note the prominent trough over Siberia and the cutoff low north of Hudson Bay.

Figures 34 and 35 are the monthly averages of the 48-hr and 96-hr forecast error for December. The heavy

dark line is the "zero" contour which encompasses the region of positive error near the pole in both plots. Quite evident is the increase in magnitude (75 m--165 m) of the positive error from the 48-hr forecast to that of 96 hours. Also evident is the extension of positive error equatorward into the vicinity of the polar troughs mentioned earlier. This is associated with the model smoothing the amplitude of the troughs (heights too high).

Figure 36 is the monthly average of the daily analyses of the 500mb height field for January 1984. A prominent trough extends equatorward over eastern Asia and a cutoff low extends south to Baffin Island. Figures 37 and 38 are the monthly averages for the 48-hr and 96-hr forecast error for January. The heavy dark line is the "zero" contour which encompasses the positive error near the pole and around the troughs in both plots. Like the error plots for the month of December, these plots illustrate the increase in magnitude of positive error with time. The extension of positive error away from the pole toward the troughs is also evident due to the model smoothing the amplitude of the trough.

b. Results of Positive Error at High Latitudes  
(NOGAPS 2.0 vs. NOGAPS 2.1)

Both NOGAPS 2.0 and NOGAPS 2.1 consistently exhibited positive error near the vicinity of the poles in the majority of the forecasts examined. The remaining cases demonstrated this error in only one hemisphere. The

large troughs which extended equatorward always displayed a positive bias in the error plots.

This positive error invariably appeared first in the shortest waves early on in the forecast. The long and planetary waves also demonstrated this error pattern at high latitudes but not as soon as the medium waves. After appearing, the positive error was seen to increase in magnitude throughout the remainder of the forecast period. This increase during the forecast seems to indicate the model is transporting more mass to the poles than it can transport equatorward.

The most obvious candidate for this source of error is the filtering technique that NOGAPS employs to maintain computational stability at high latitudes. No changes were made to this filtering process in the newer model version. There was no decrease in positive error noted at the poles for NOGAPS 2.1. The model upgrade in NOGAPS 2.1 did appear to improve forecast skill somewhat with respect to amplitude smoothing. However, the continued positive error near the poles and in the polar troughs would indicate the filtering process is largely responsible for this pattern of error.

### 3. Major Non-Systematic Error

In the eight forecasts examined for NOGAPS 2.1, no evidence of the difficulty encountered by the older model version in forecasting the flow downstream of North America

was noted. As far as could be determined, NOGAPS 2.1 did not exhibit this type or any other non-systematic error approaching the magnitude of that noted for NOGAPS 2.0.

#### IV. CONCLUSIONS AND RECOMMENDATIONS

In this study a total of twelve NOGAPS 500mb 5-day forecasts were verified by employing spectral decomposition. Eleven forecasts were from the winter of 1983-84 and one from the spring of 1983. Four forecasts were for the NOGAPS 2.0 (six-layer) model version and eight for the NOGAPS 2.1 (nine-layer) model version. Spectral analysis was utilized to decompose the forecast and observed 500mb wave fields into wavenumber components. These wavenumbers were then placed into planetary (WN 1-2), long (WN 4-7) and medium (WN 8-12) wavenumber groupings.

Each forecast (24, 48, 72, 96 and 120-hr) was then compared to the corresponding analysis (same wavenumber group) to gain insight into the source of error. In addition, error plots for each forecast time increment were used to determine the magnitude of error. Hovmoller diagrams for each wavenumber group were employed to analyze error initiation and magnitude with respect to that of the other wavenumber groups. In this manner any "cascading" of error (up or down) throughout the wave spectrum could be ascertained both temporally and spatially.

Two patterns of error clearly emerged in both NOGAPS model versions. The first error pattern was the amplitude smoothing (or dampening) of planetary, long and medium wave

features. The inability of either model version to correctly depict adequate troughing and ridging was seen in all wave number groups. The second error pattern noted was smoothing of the polar trough and consistent positive error at high latitudes. This positive error over the poles and in the polar trough was seen to increase (in magnitude) during the forecast period.

The model upgrade from six to nine vertical sigma levels appears to have improved NOGAPS 2.1 500mb forecasts. The reduction in the 500mb amplitude error and slower error growth supports this conclusion. The disproportionate amount of error contributed from the long waves was surprising. In several instances, both models' long wave forecasts were poor. This loss of amplitude and resultant smoothing toward the end of the forecast period seem to indicate an erroneous transfer of eddy kinetic energy to zonal kinetic energy.

NOGAPS 2.1 appeared to have no effect on the positive error at the poles and in the polar troughs. The filtering technique employed to maintain computational stability at high latitudes may mask any forecast improvement in this region.

One NOGAPS 2.0 forecast (4-9 November 1983) encountered major problems in forecasting the 500mb flow downstream of North America. By 48 hours the older model version had begun filling a low which had developed into a cutoff low over the Maritime Provinces. Downstream the model was

unable to depict the increasing low-index flow of the medium and long wave features.

By mid-period the planetary waves downstream experienced the same pattern of error. The 72-hr forecast had depicted zonal flow in all wave groups when the opposite was observed. By the end of the forecast the model began to reflect the low-index flow noted 48 hours earlier, but a large trough over the Atlantic Ocean and blocking ridge over Europe were absent. Noteworthy is the fact that the model also mishandled a case of maritime cyclogenesis in the Atlantic Ocean during the forecast period. It is difficult to determine if this system was poorly forecast due to the lack of upper-level support or developed in the lower troposphere and contributed to 500mb level model error over Europe.

This error was also noted in NOGAPS 2.0 for the 24-29 November forecast. It occurred over the same region but did not approach the magnitude of error for the 4-9 November case. Unlike the 4-9 November forecast, no simultaneous development of maritime cyclogenesis in a nearby region was noted. This would seem to indicate that the maritime cyclogenesis did contribute to the upper-level error. However, the method of analysis employed in this study does not conclusively show this as only one level (500mb) was examined.

This type of error was not observed in any of the NOGAPS 2.1 forecasts. Considering the increased sample size (eight

vs. four) of forecasts examined, the absence of this particular error would tend to indicate model improvement. Coupling this with the model success in reducing amplitude smoothing error would further suggest that forecast skill has been improved.

Although not cited as a major source of error, NOGAPS 2.1 exhibited notable improvement over NOGAPS 2.0 in forecasting the correct axis tilt of the various scale wave features. NOGAPS 2.0 would frequently depict insufficient axis tilt and on numerous occasions incorrect tilt of the wave feature axis was noted. NOGAPS 2.1, on the other hand, was superior in that the occurrence of insufficient and incorrect axis tilt was markedly reduced.

With respect to amplitude smoothing, NOGAPS 2.1 demonstrated limited success in two ways:

- a. The magnitude of error was reduced by 10-15 percent.
- b. The growth of sizeable error occurred approximately 18-24 hours later in the forecast compared to that of NOGAPS 2.0.

Recommendations for further research as a result of this study include the following:

1. As more NOGAPS 2.1 data become available, increase the sample size and employ statistical methods to facilitate identifying systematic (vice random) error.
2. In the same vein utilize climatology (e.g. monthly averages of forecast error) along with spectral analysis

and Hovmoller diagrams to isolate error sources within the various wavenumber groups.

3. Apply spectral analysis and Hovmoller diagrams to multiple levels (upper, middle and low) for the same forecast period. Assuming vertical coupling of the upper atmosphere to that of the surface, forecast error at various levels can be analyzed to determine model strengths and weaknesses.

The viability of the analysis methods employed in this study demonstrate the utility of spectral decomposition techniques and Hovmoller diagrams for future research into operational numerical prediction models. If the objective of longer range model prediction is to be accomplished, verification methods employed in this study coupled with the recommendations above can isolate model strengths and weaknesses.

APPENDIX A

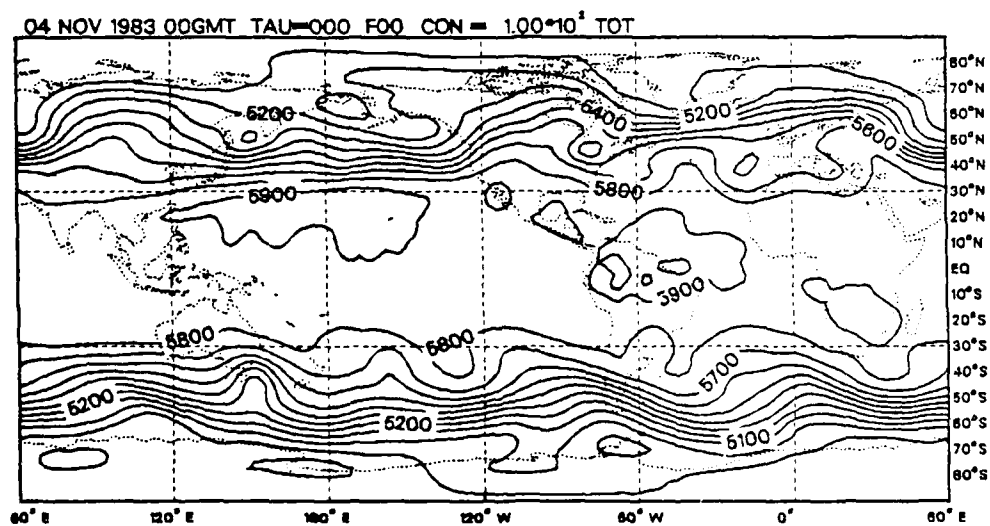


Figure 1. 4 November 1983 Analysis of Total Wave Field (Contour Interval = 100 m)

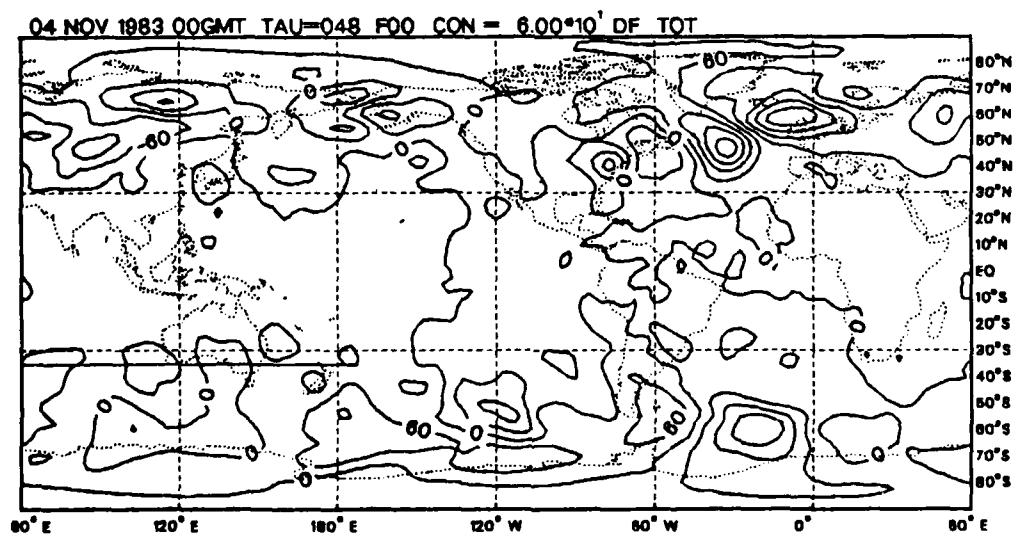


Figure 2. 4 November 1983 48-hr Forecast Error of  
Total Waves (Contour Interval = 60 m)

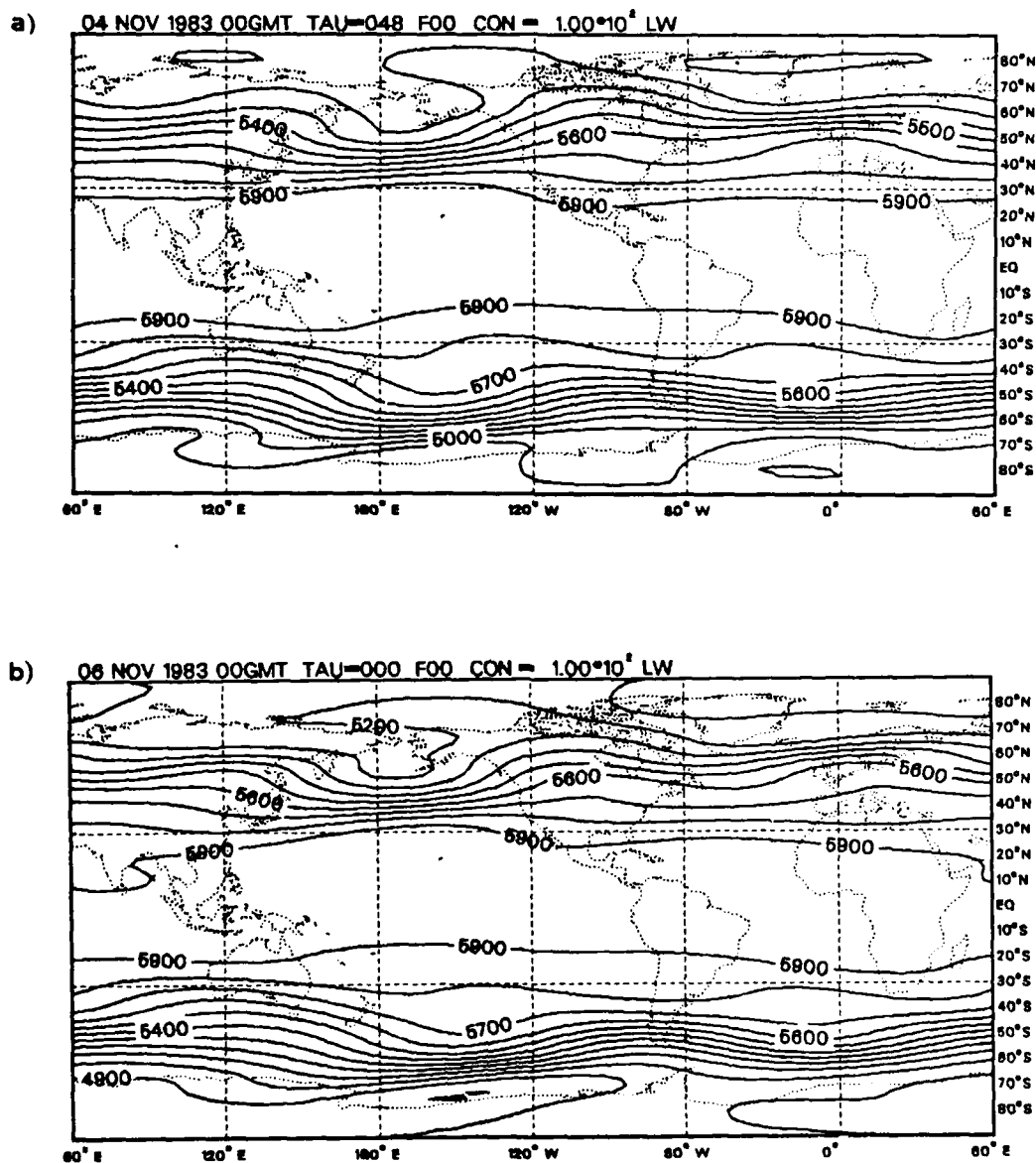


Figure 3. a) 4 November 1983 48-hr Planetary Wave Forecast and b) Corresponding Analysis for 6 November 1983

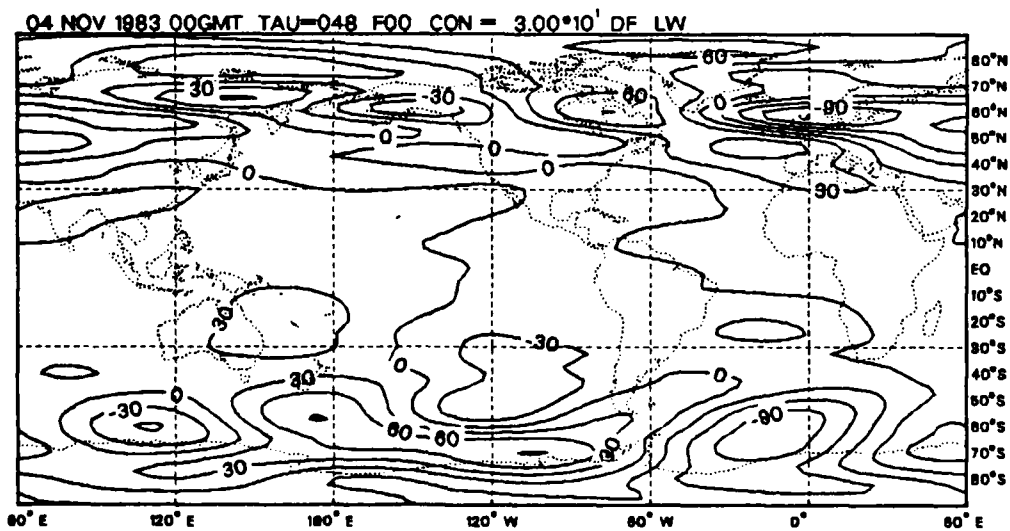


Figure 4. 4 November 1983 48-hr Planetary Wave Forecast Error (Contour Interval = 30 m)

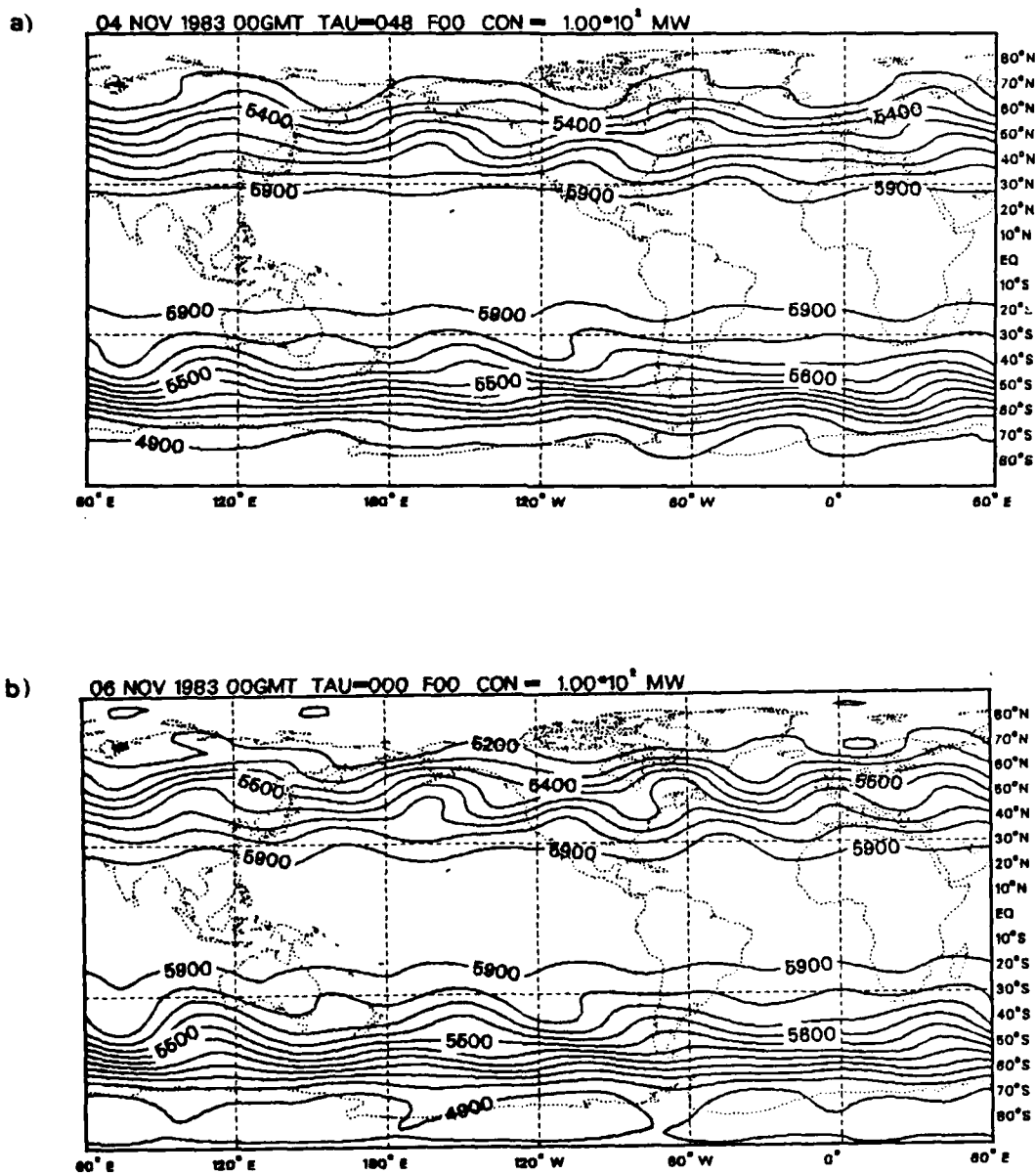


Figure 5. a) 4 November 1983 48-hr Long Wave Forecast and b) Corresponding Analysis for 6 November 1983 (Contour Interval = 100 m)

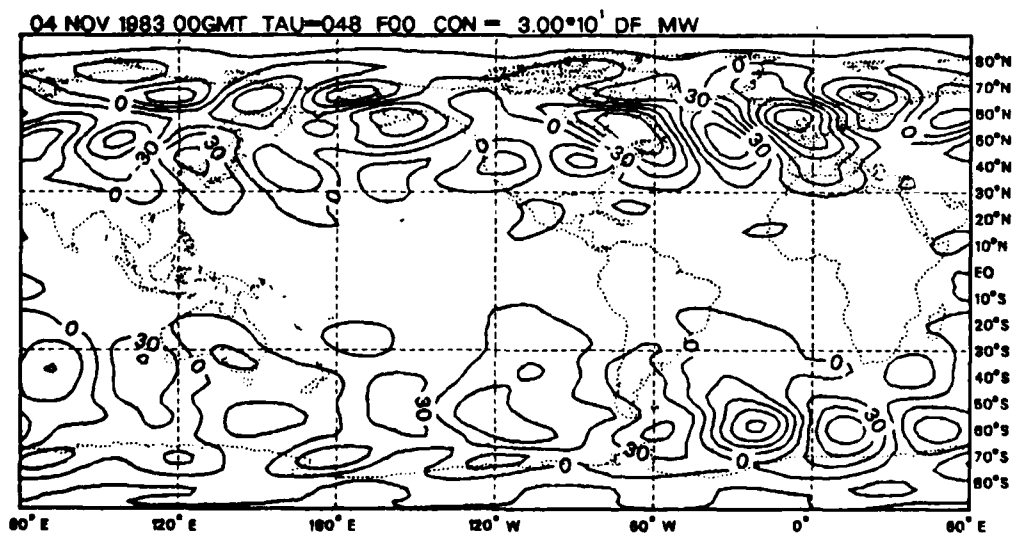


Figure 6. 4 November 1983 48-hr Long Wave Forecast Error (Contour Interval = 30 m)

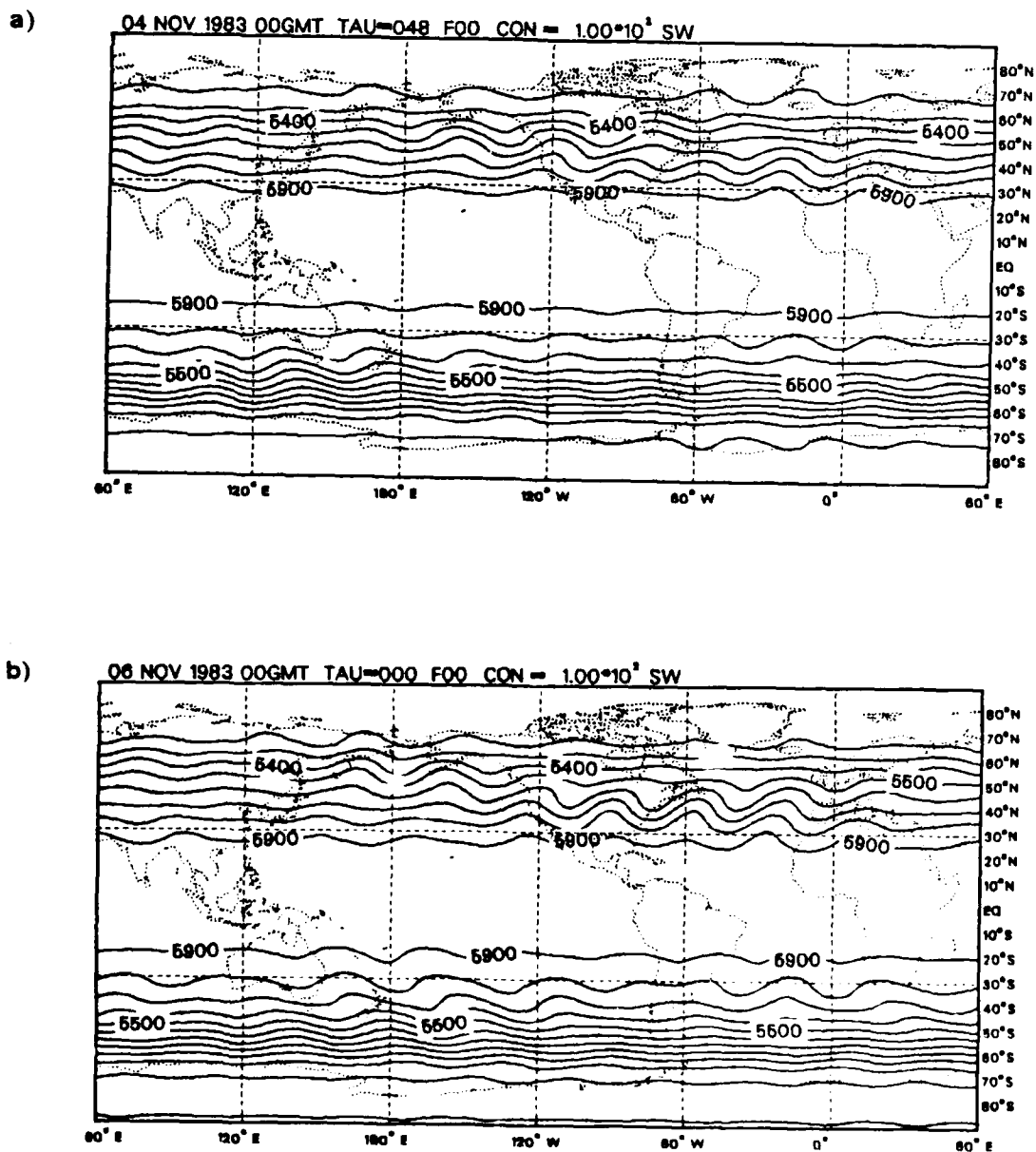


Figure 7. a) 4 November 1983 48-hr Medium Wave Forecast and b) Corresponding Analysis for 6 November 1983 (Contour Interval = 100 m)

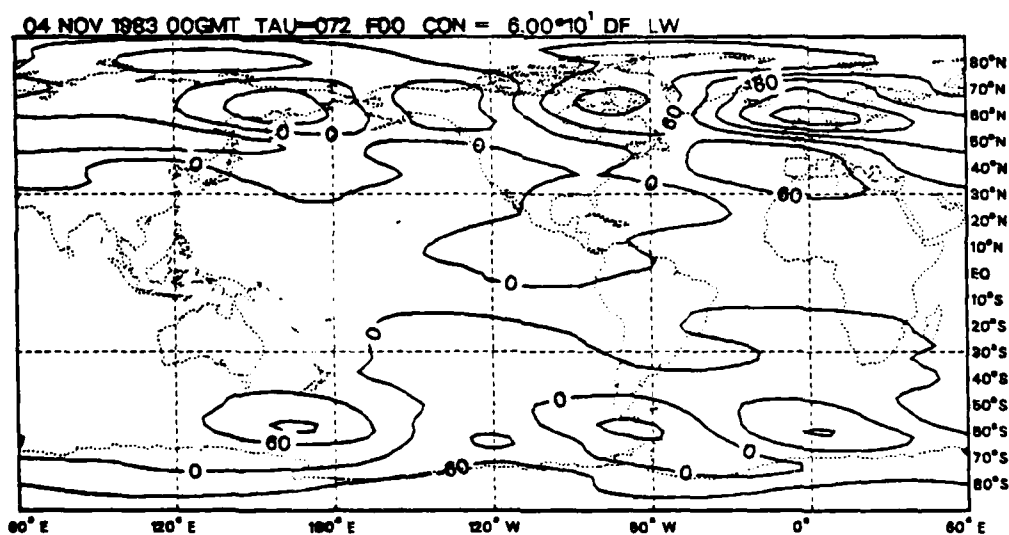


Figure 8. 4 November 1983 72-hr Planetary Wave  
Forecast Error (Contour Interval = 60 m)

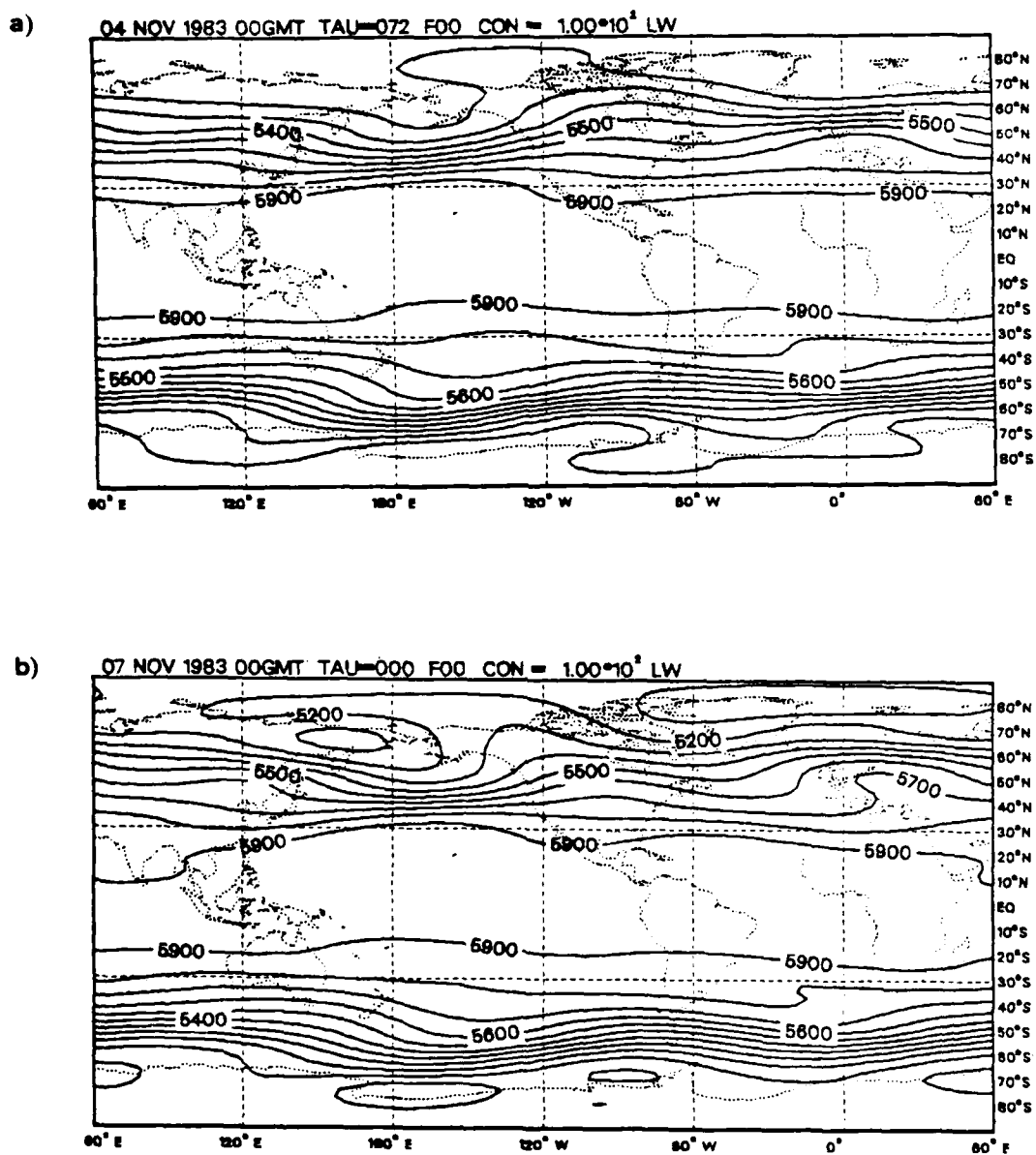


Figure 9. a) 4 November 1983 72-hr Planetary Wave Forecast and b) Corresponding Analysis (Contour Interval = 100 m)

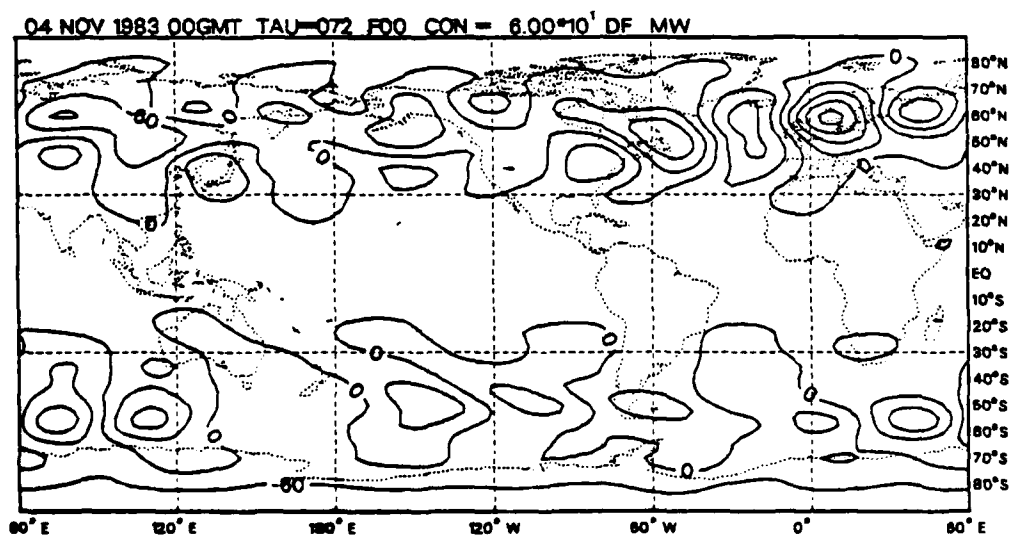


Figure 10. 4 November 1983 72-hr Long Wave Forecast Error (Contour Interval = 60 m)

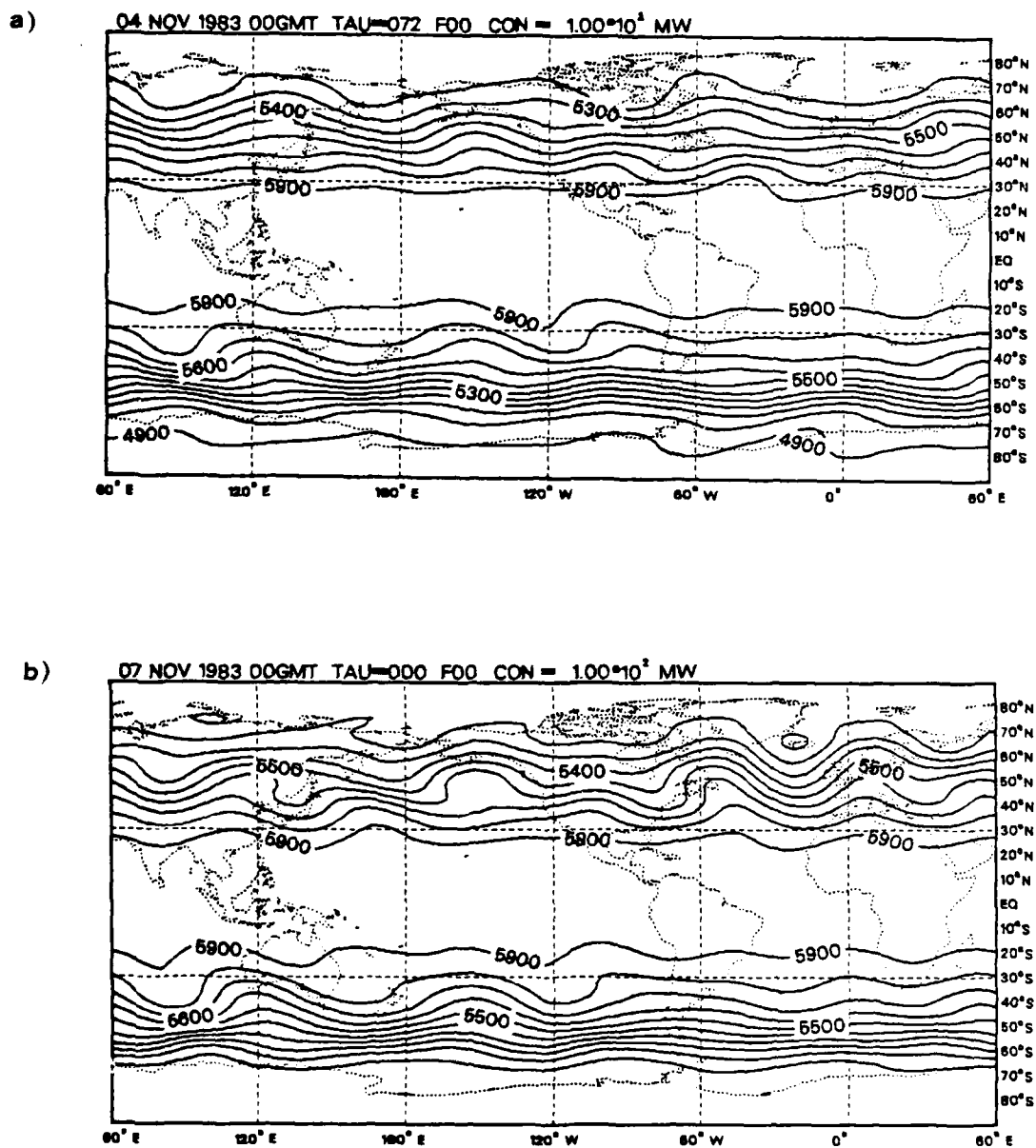


Figure 11. a) 4 November 1983 72-hr Long Wave Forecast and b) Corresponding Analysis (Contour Interval = 100 m)

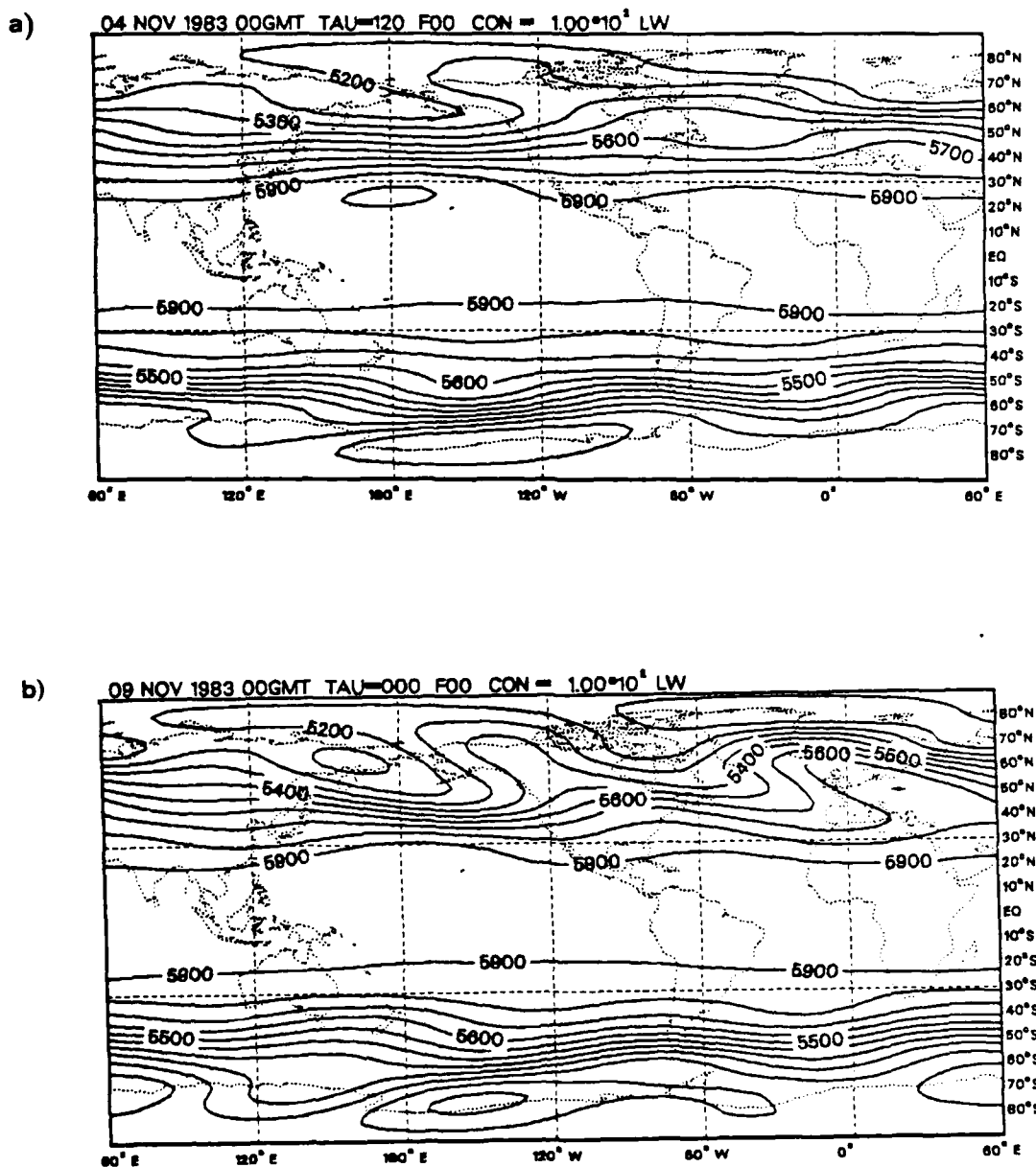


Figure 12. a) 4 November 1983 120-hr Planetary Wave Forecast and b) Corresponding Analysis (Contour Interval = 100 m)

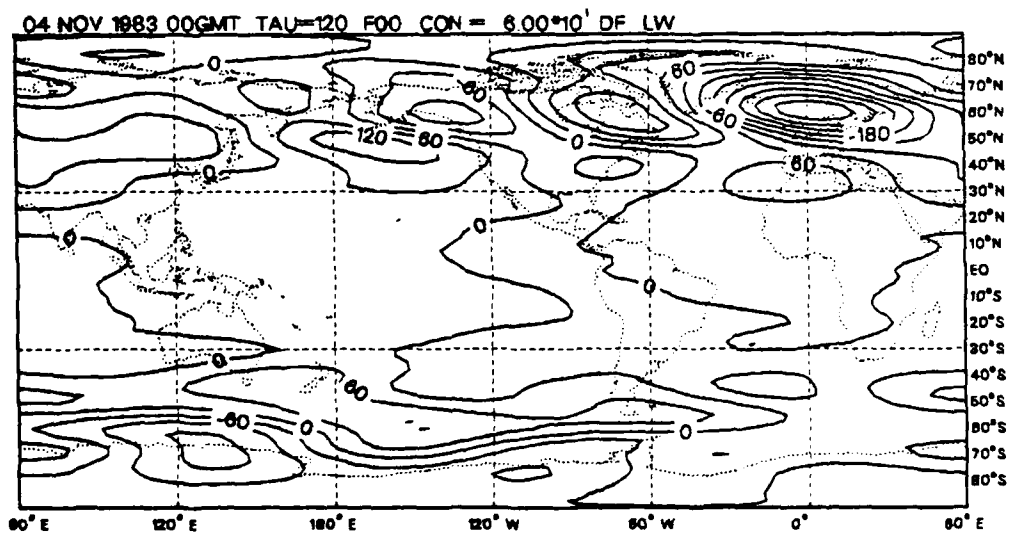


Figure 13. 4 November 1983 120-hr Planetary Wave  
Forecast Error (Contour Interval = 60 m)

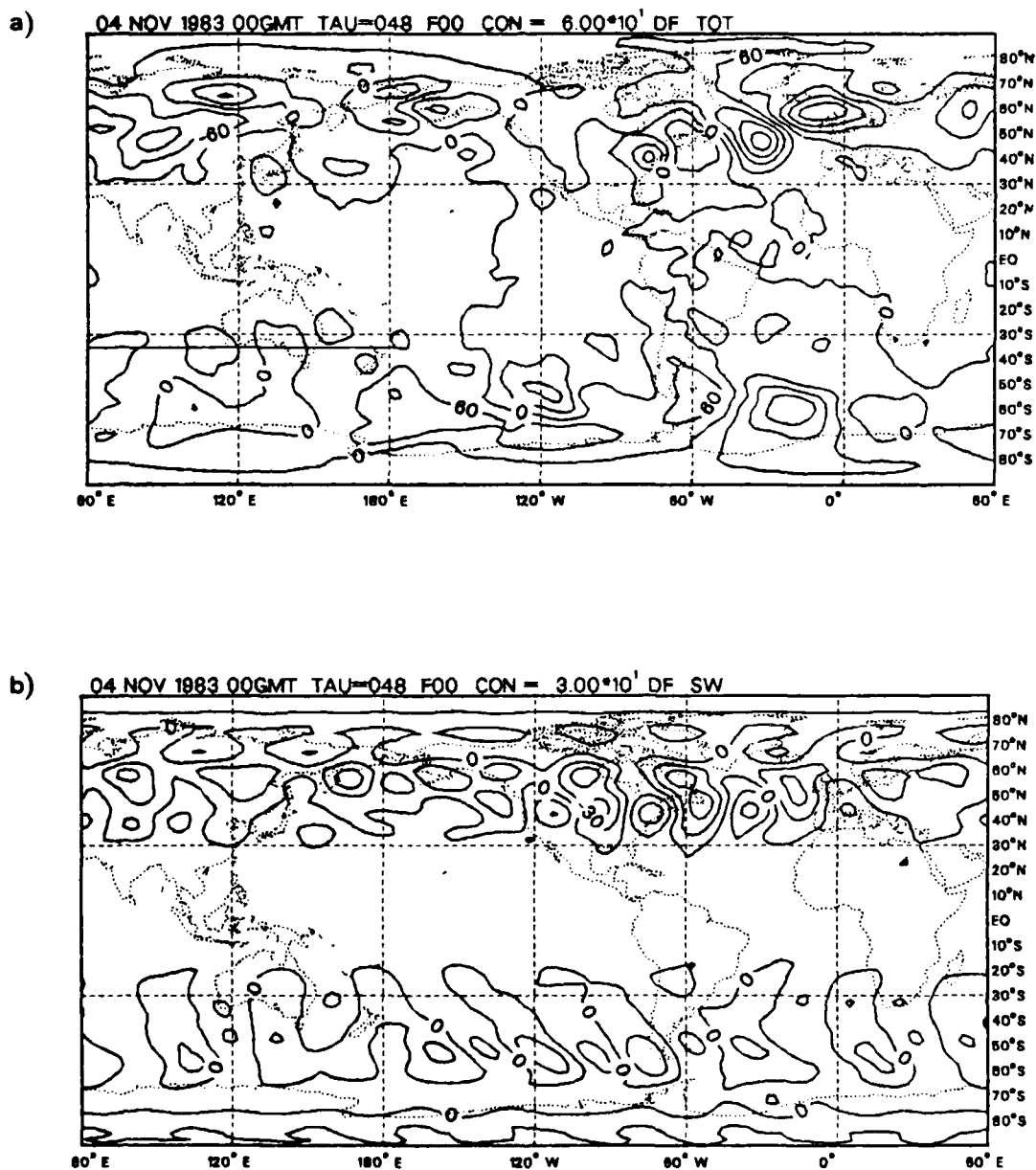


Figure 14. a) 4 November 1983 48-hr Total Forecast Error (Contour Interval = 60 m) and b) 48-hr Medium Wave Forecast Error (Contour Interval = 30 m)

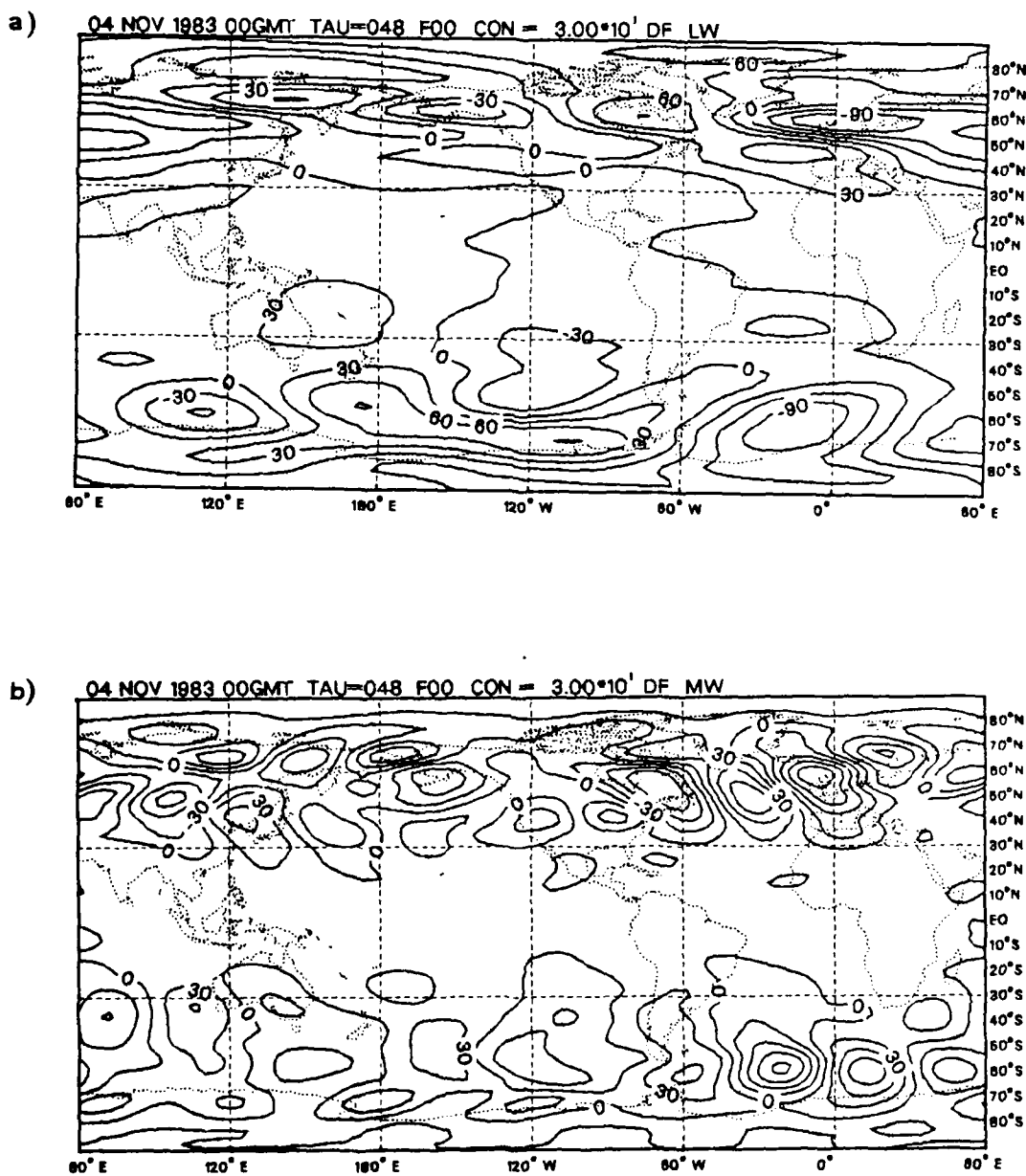


Figure 15. 4 November 1983 48-hr Forecast Error for  
a) Planetary Waves and b) Long Waves  
(Contour Interval = 30 m)

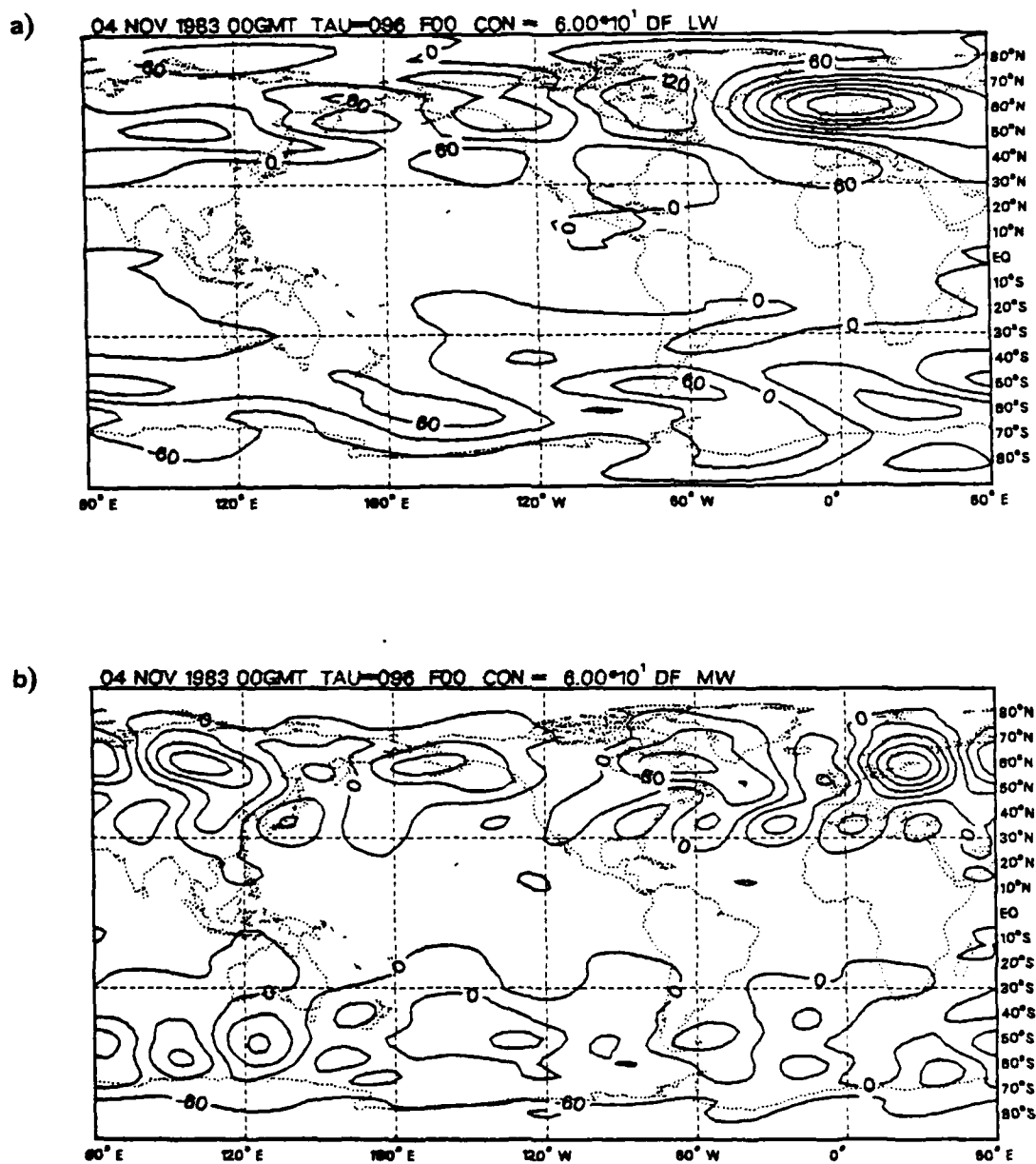


Figure 16. 4 November 1983 96-hr Forecast Error for  
a) Planetary Waves and b) Long Waves  
(Contour Interval = 60 m)

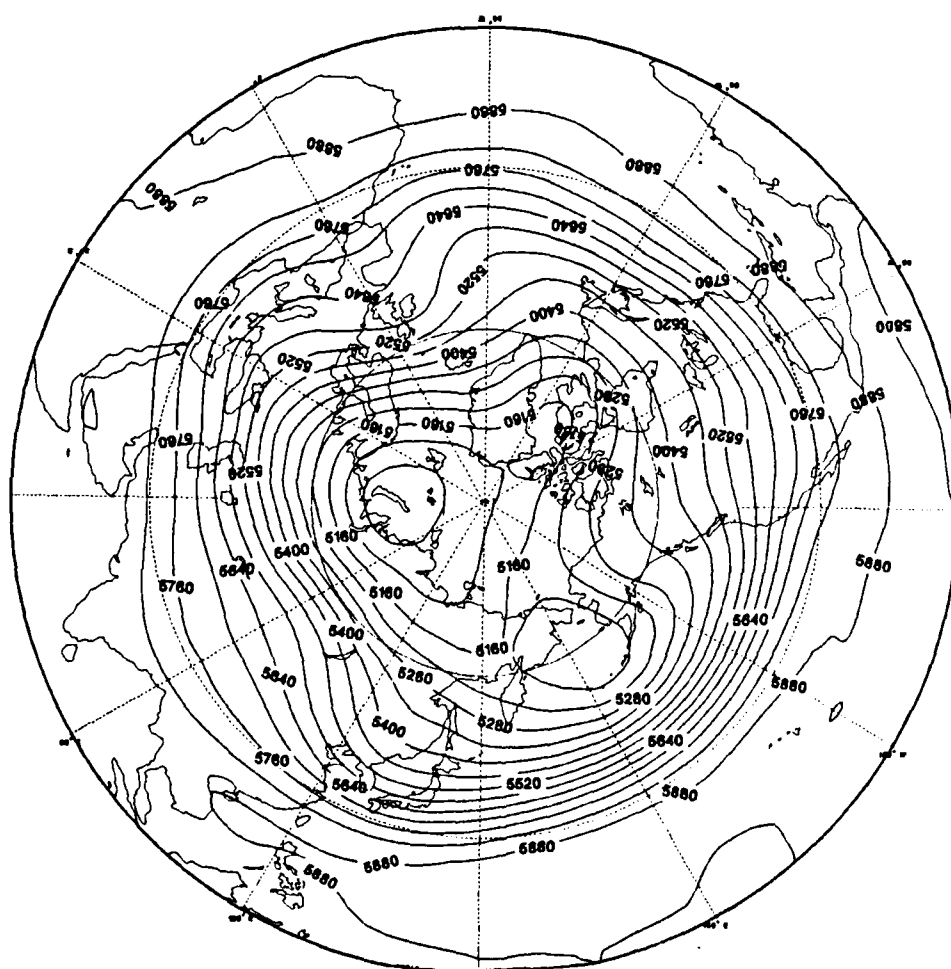


Figure 17. Polar Stereographic Plot of Average Height Field for Month of November (Contour Interval = 60 m)

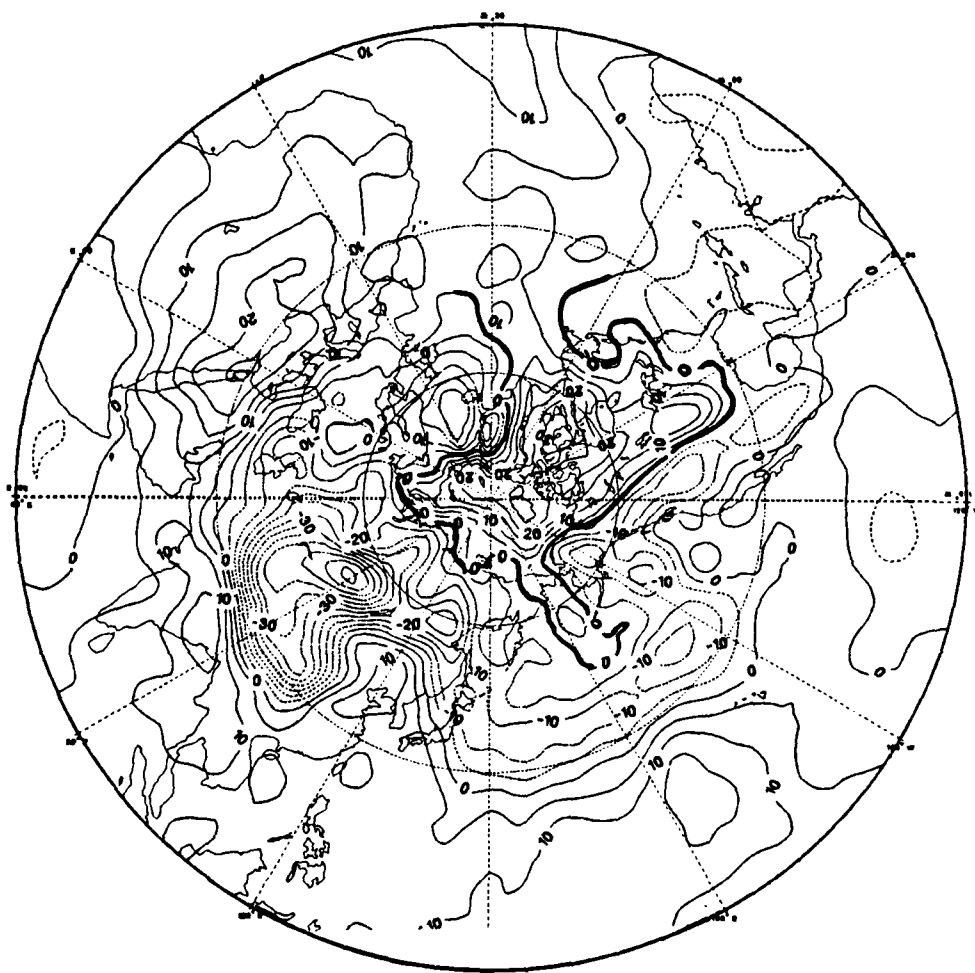


Figure 18. Polar Stereographic Plot of 24-hr Average  
Forecast Error for November 1983  
(Contour Interval = 5 m)

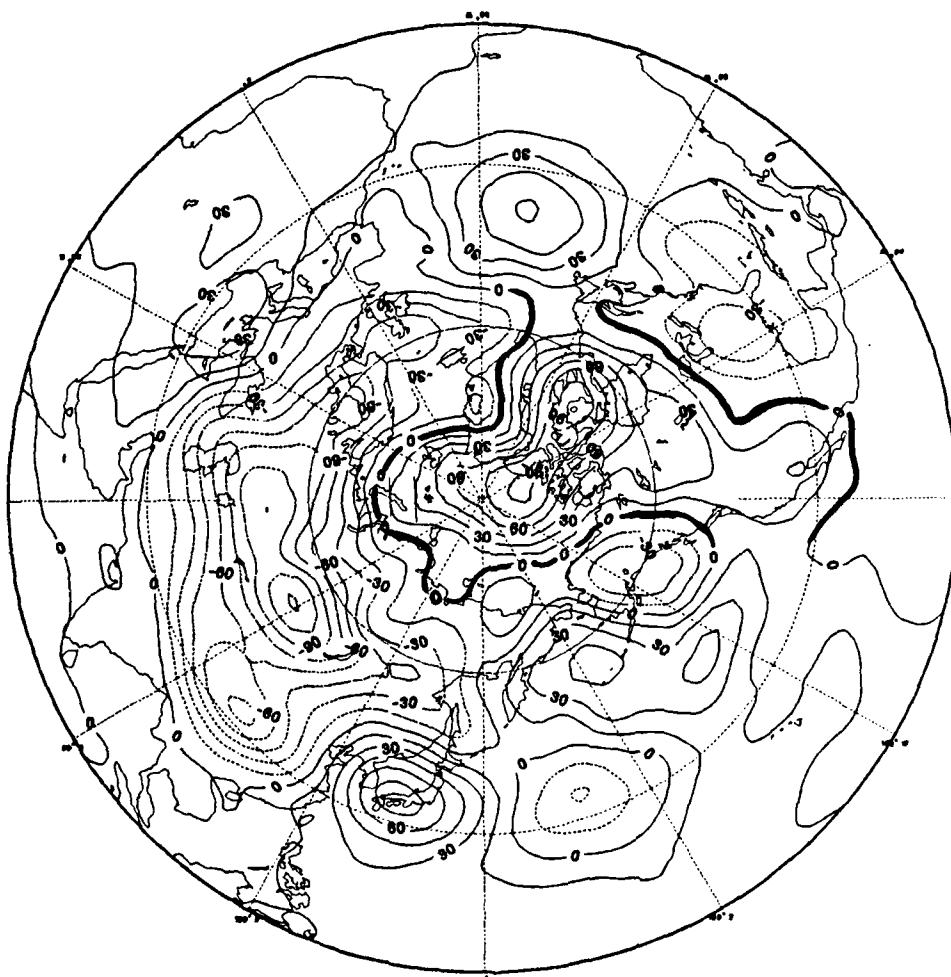


Figure 19. Polar Stereographic Plot of 96-hr Average  
Forecast Error for November 1983  
(Contour Interval = 15 m)

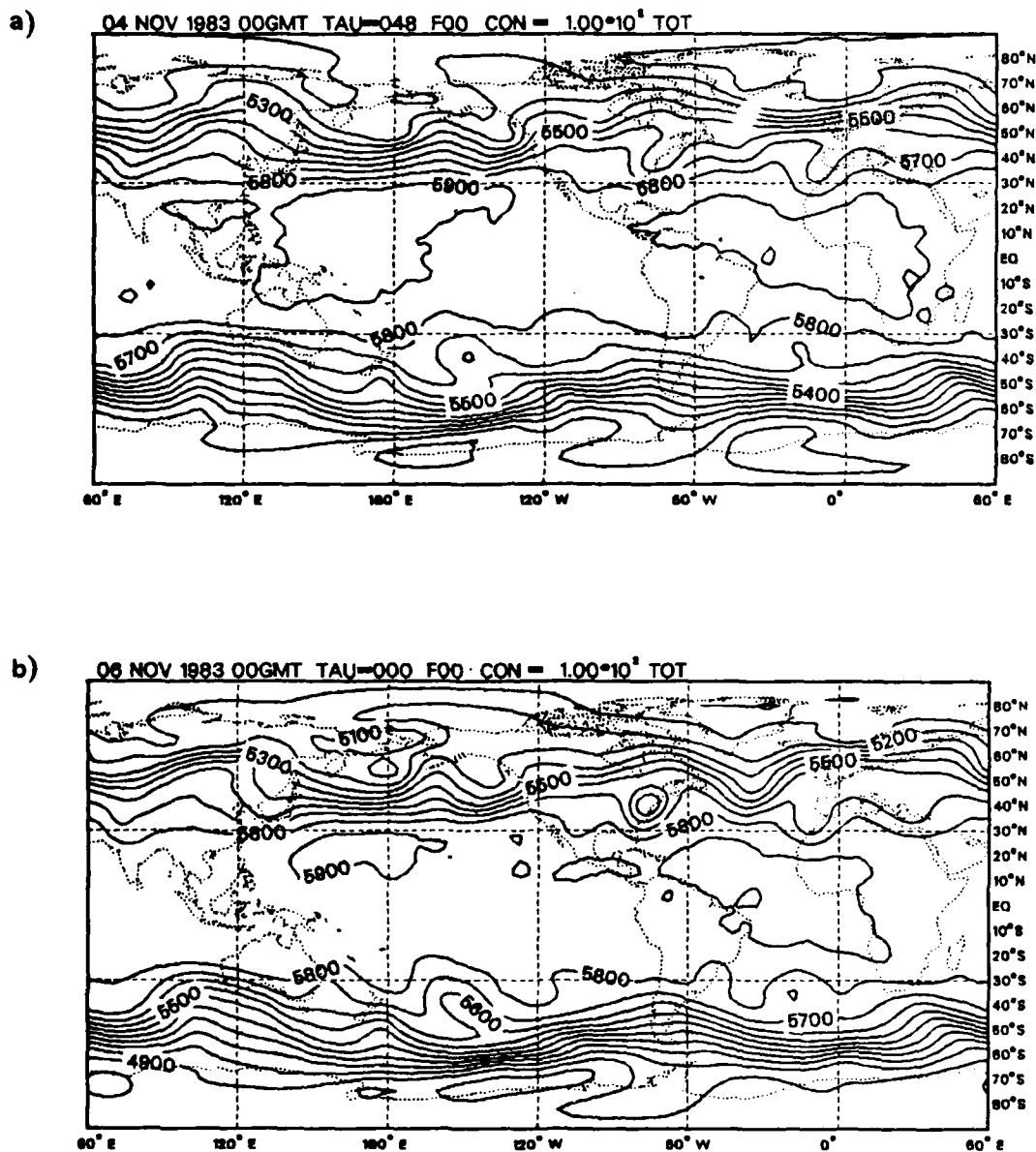


Figure 20. a) 4 November 1983 48-hr Total Wave Forecast and b) Corresponding Analysis (Contour Interval = 100 m)

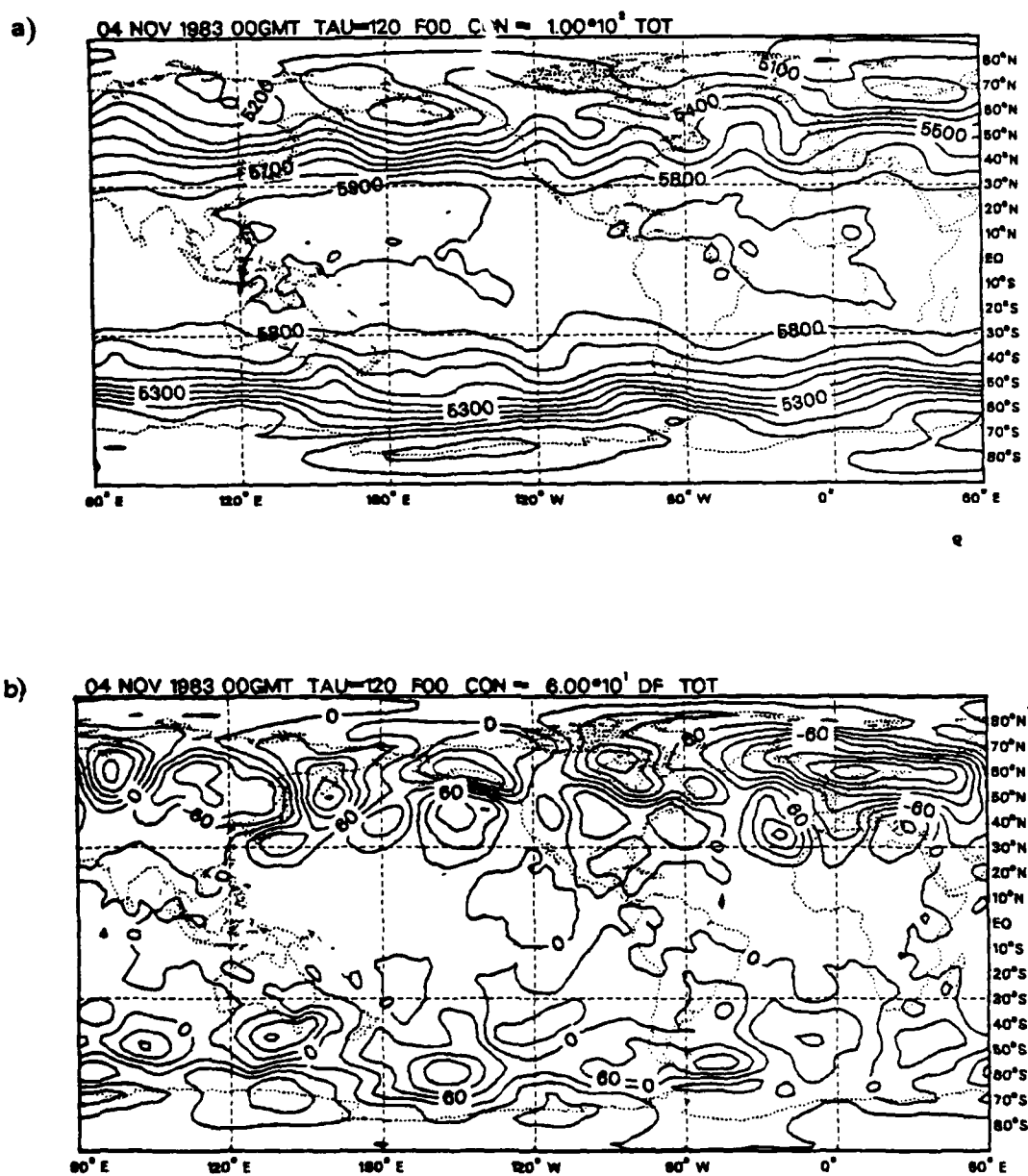


Figure 21. a) 4 November 1983 120-hr Total Wave Forecast (Contour Interval = 100 m) and  
b) Total Error (Contour Interval = 60 m)

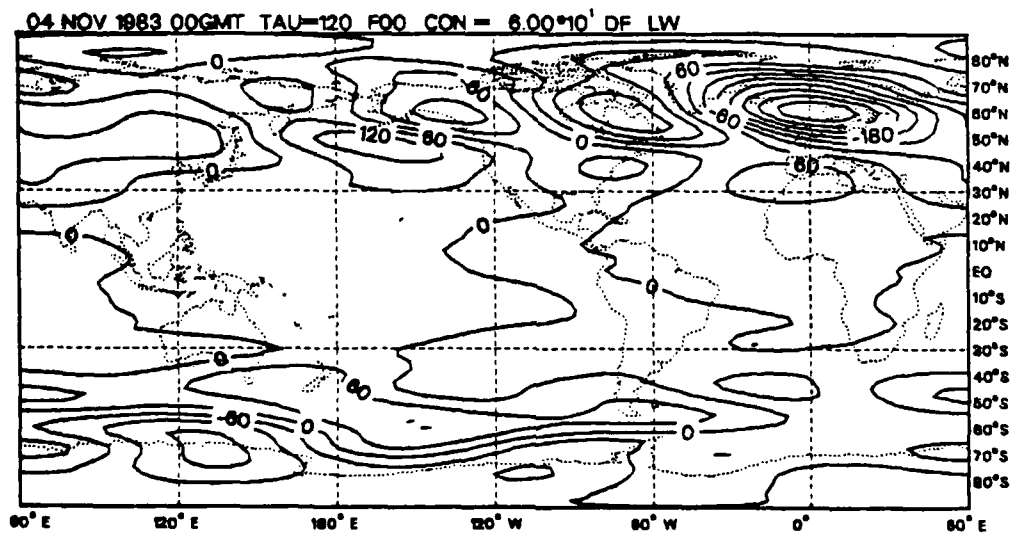


Figure 22. 4 November 1983 120-hr Planetary Wave Forecast Error (Contour Interval = 60 m)

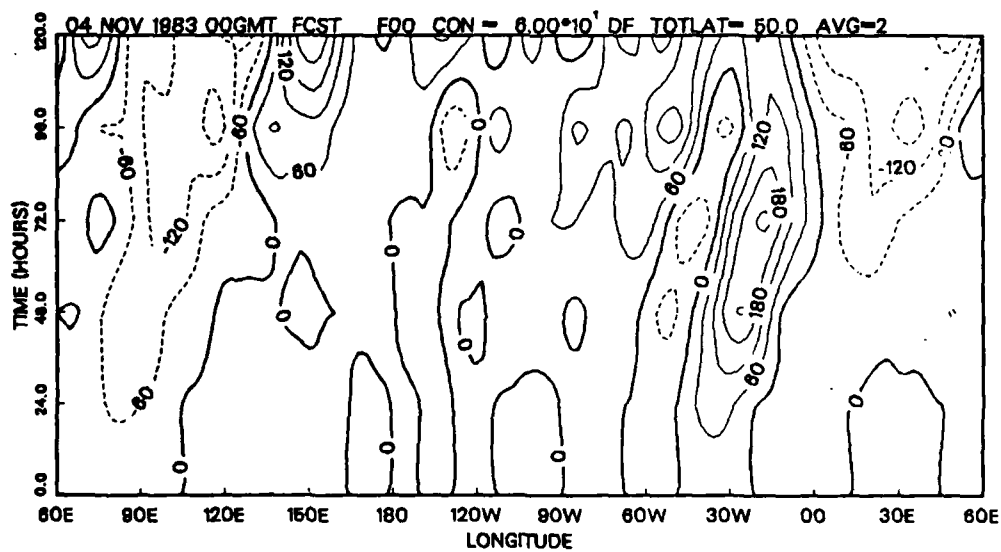


Figure 23. Hovmoller Diagram at 50° N of Total Forecast Error for 4-9 November 1983 (Contour Interval = 60 m)

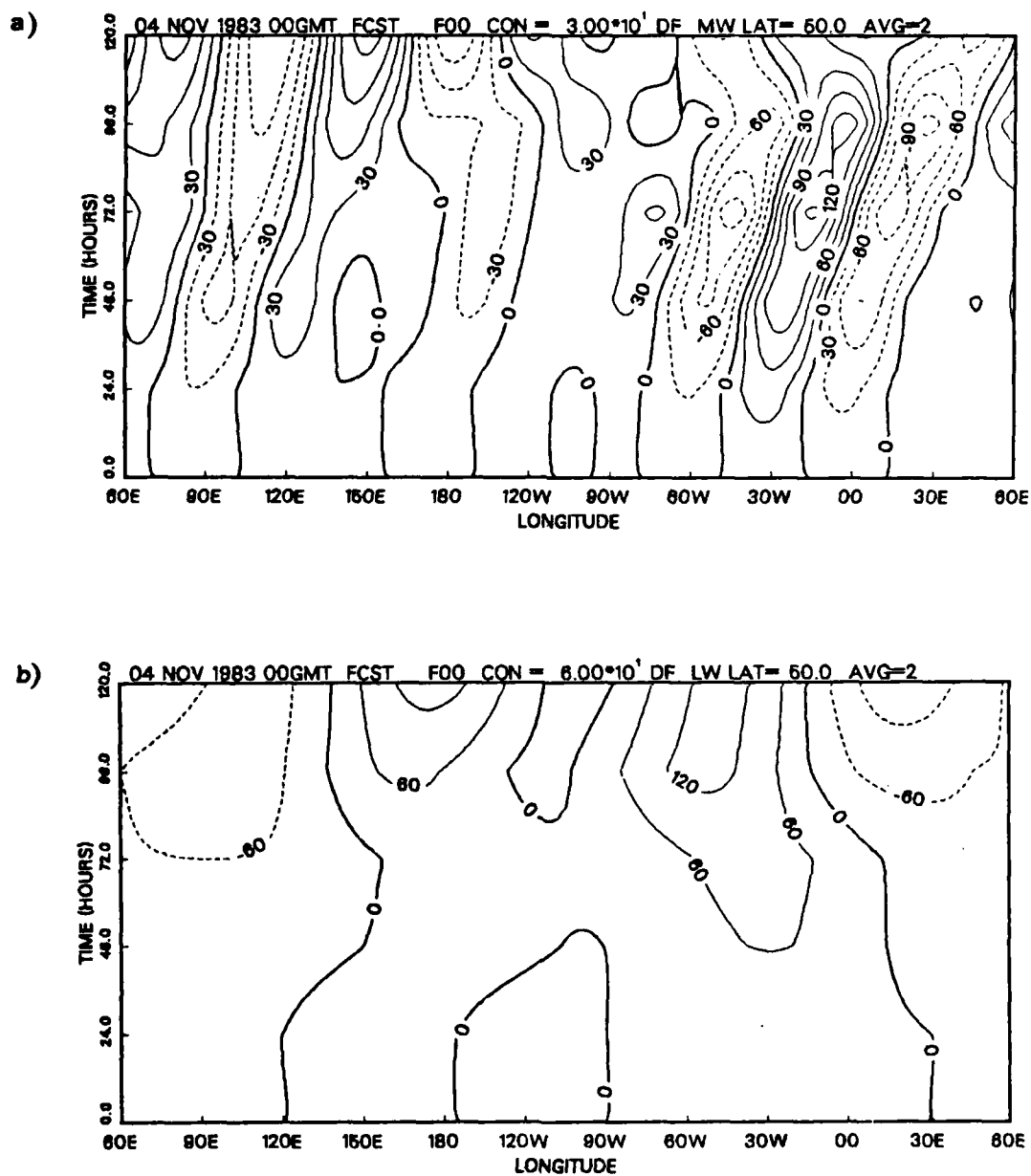


Figure 24. Hovmoller Forecast Error Diagrams at 50° N of a) Long Waves (Contour Interval = 30 m) and b) Planetary Waves (Contour Interval = 50 m) for 4-9 November 1983

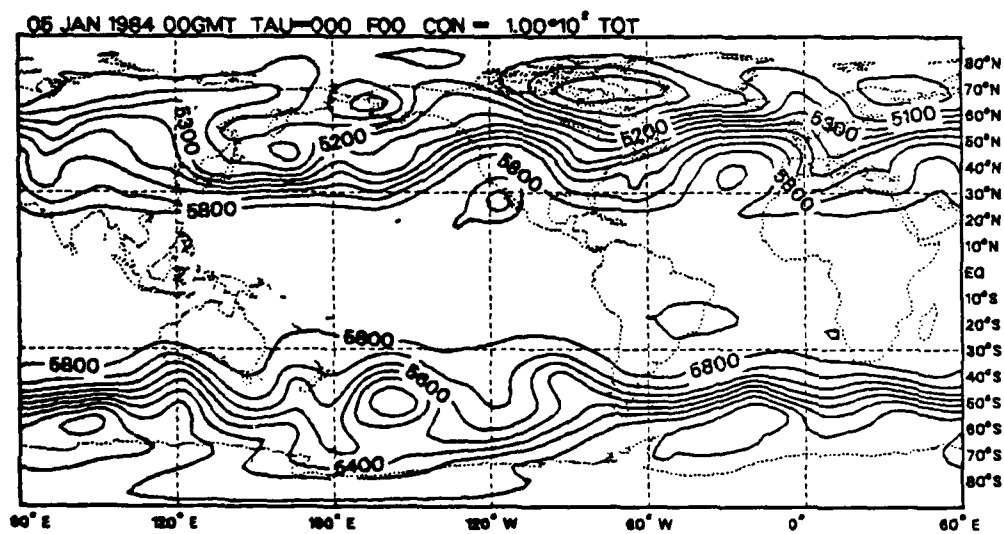


Figure 25. 5 January 1984 Analysis of Total Wave Field (Contour Interval = 100 m)

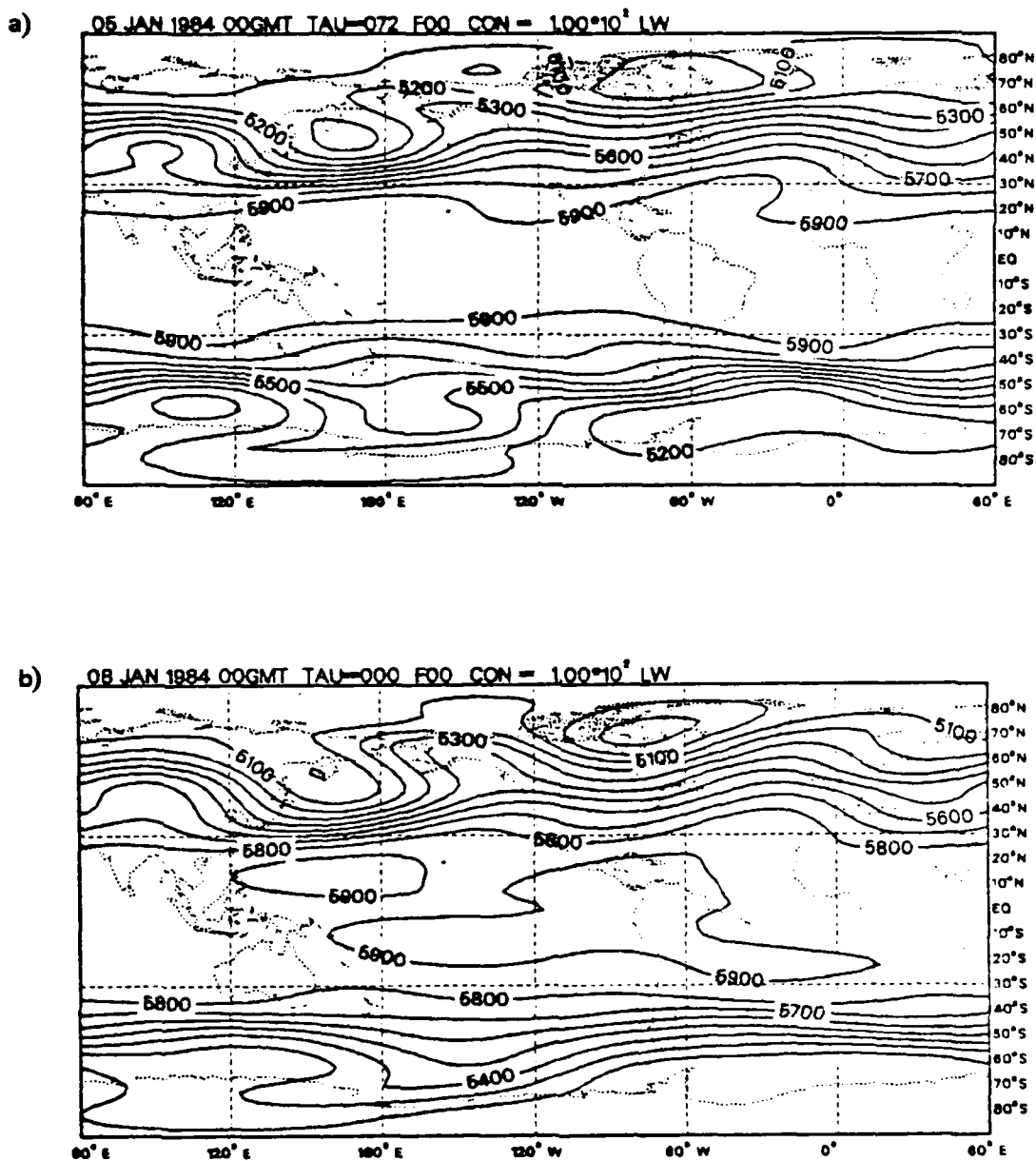


Figure 26. a) 5 January 1984 72-hr Planetary Wave Forecast and b) Corresponding Analysis for 8 January 1984 (Contour Interval = 100 m)

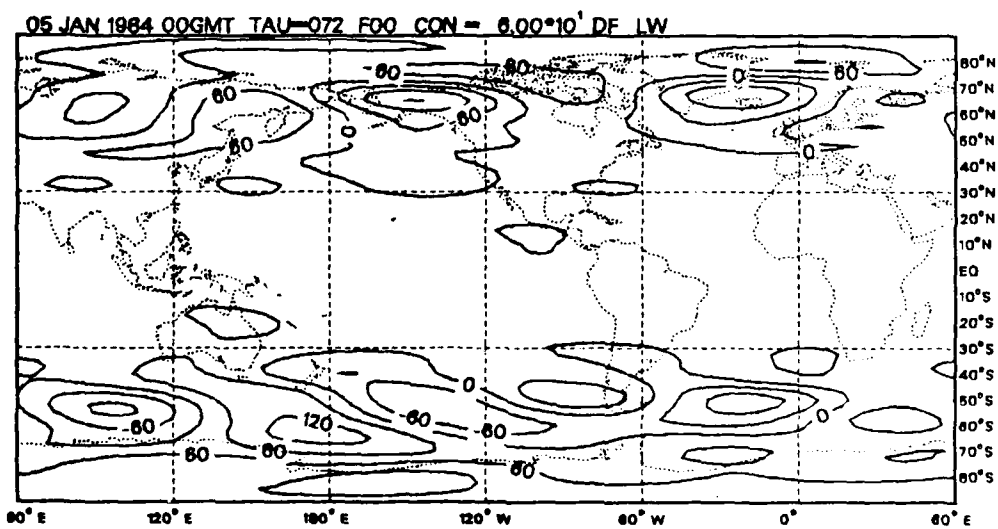


Figure 27. 5 January 1984 72-hr Planetary Wave Forecast Error (Contour Interval = 60 m)

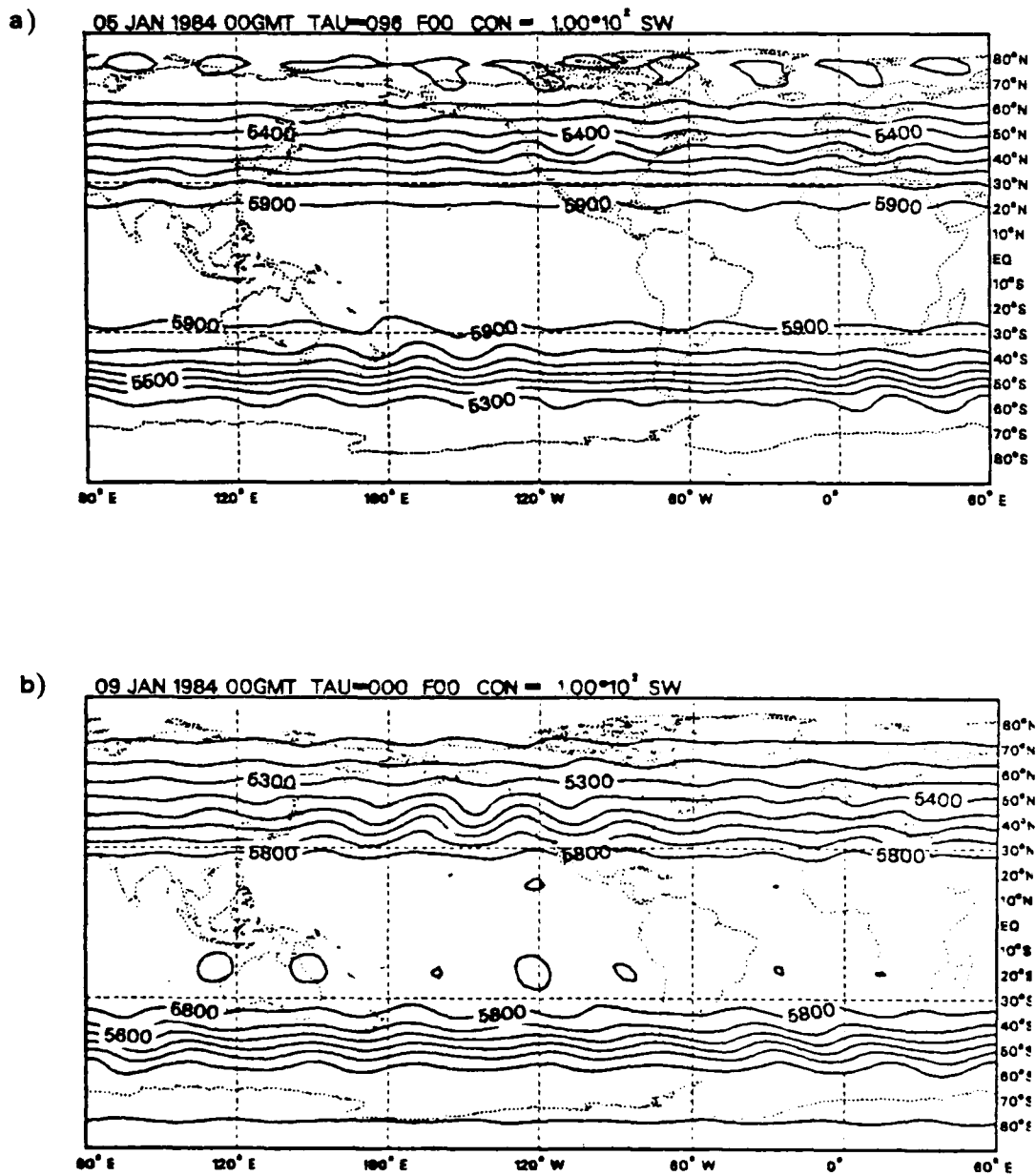


Figure 28. a) 5 January 1984 96-hr Medium Wave Forecast and b) Corresponding Analysis (Contour Interval = 100 m)

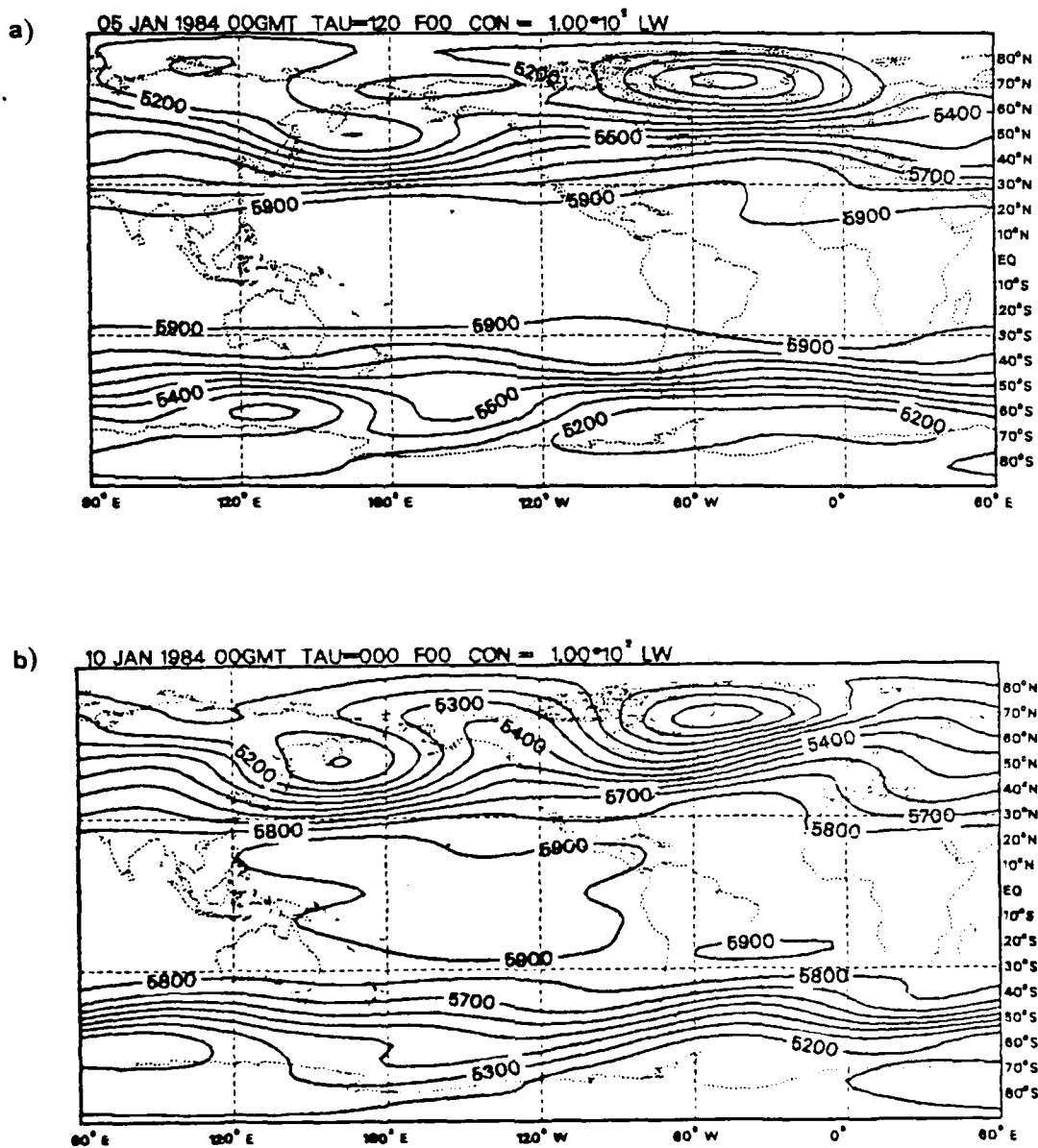


Figure 29. a) 5 January 1984 120-hr Planetary Wave Forecast and b) Corresponding Analysis (Contour Interval = 100 m)

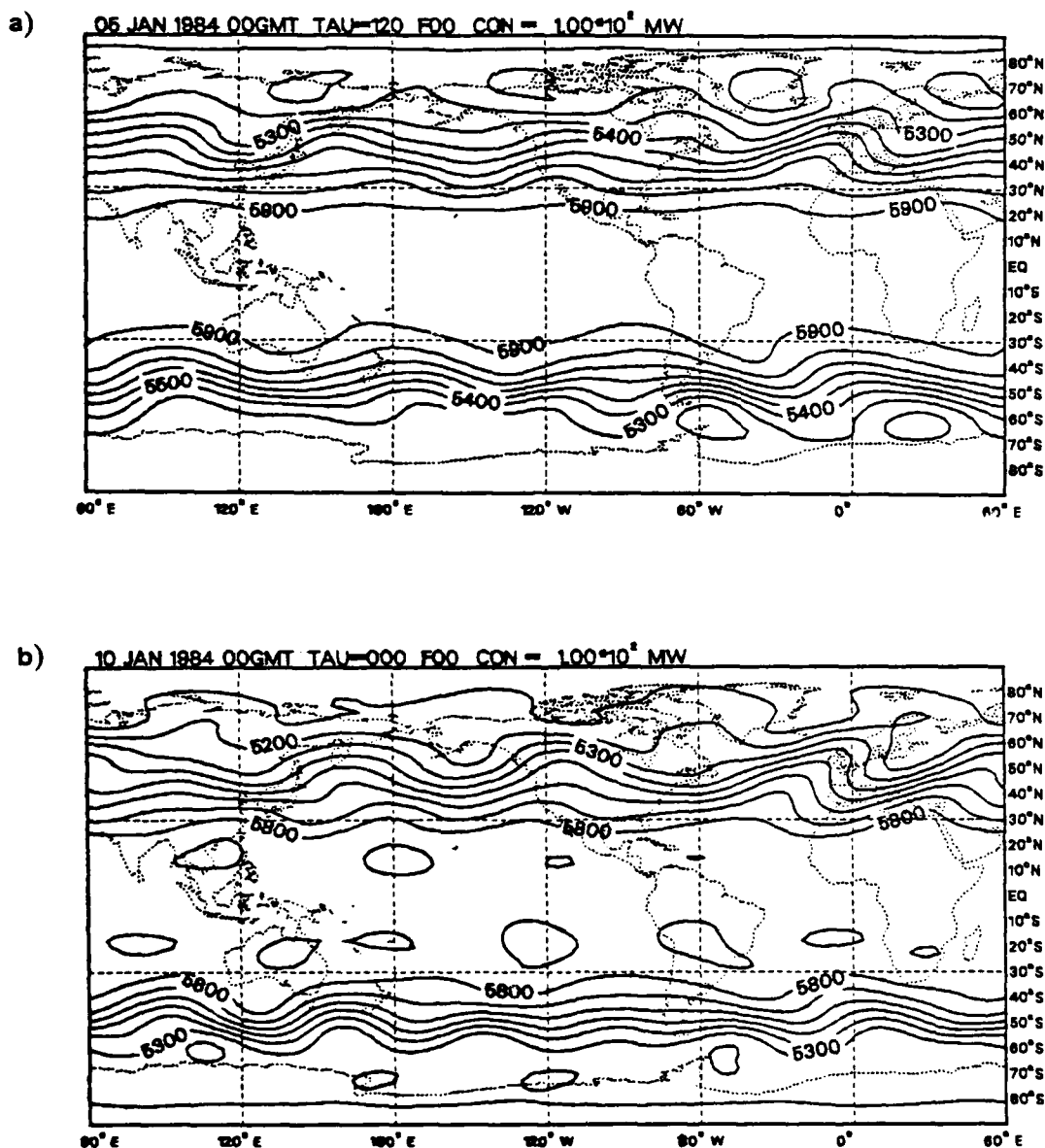


Figure 30. a) 5 January 1984 120-hr Long Wave Forecast and b) Corresponding Analysis (Contour Interval = 100 m)

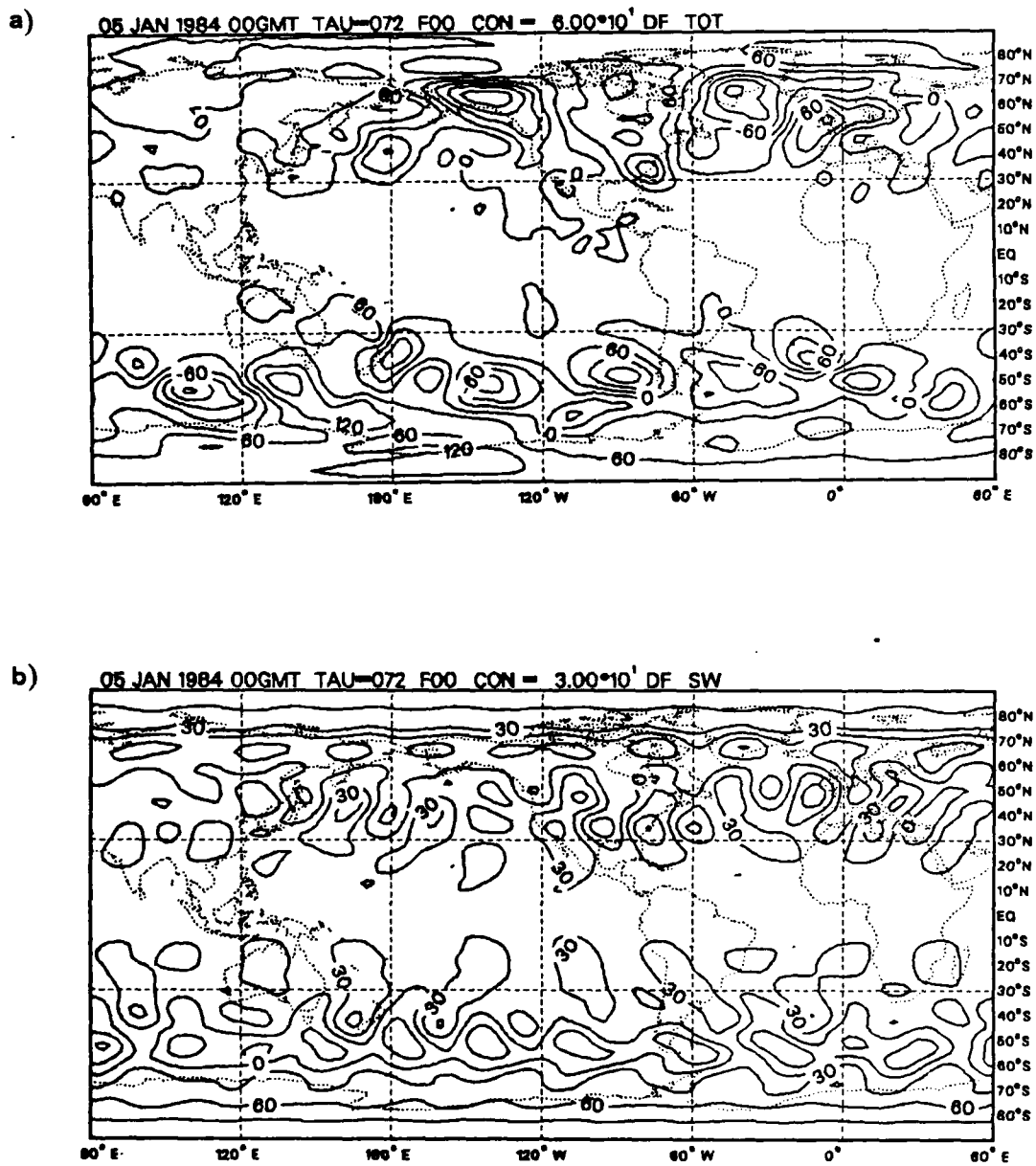


Figure 31. 5 January 1984 72-hr Forecast Error for  
a) Total Waves (Contour Interval = 60 m)  
and b) Medium Waves (Contour Interval = 30 m)

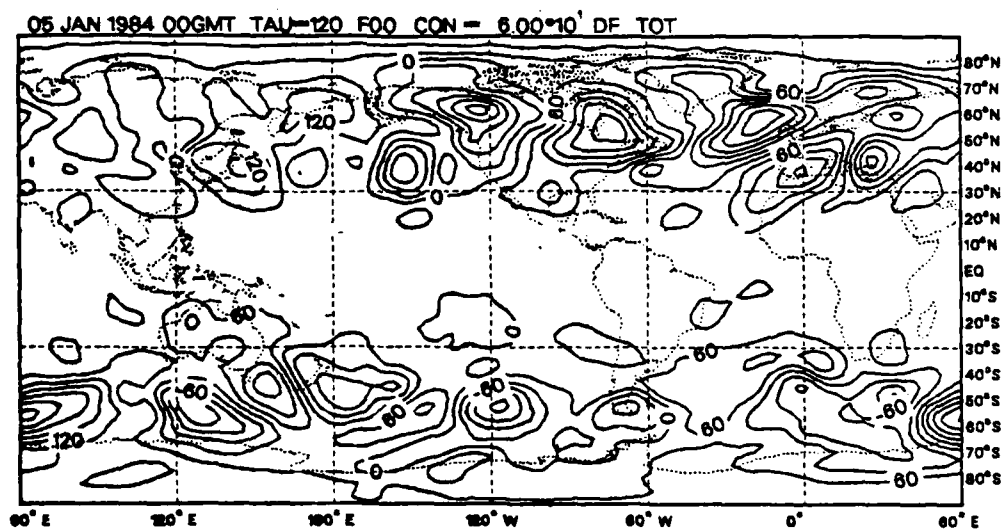


Figure 32. 5 January 1984 120-hr Forecast Error for Total Waves (Contour Interval = 60 m)

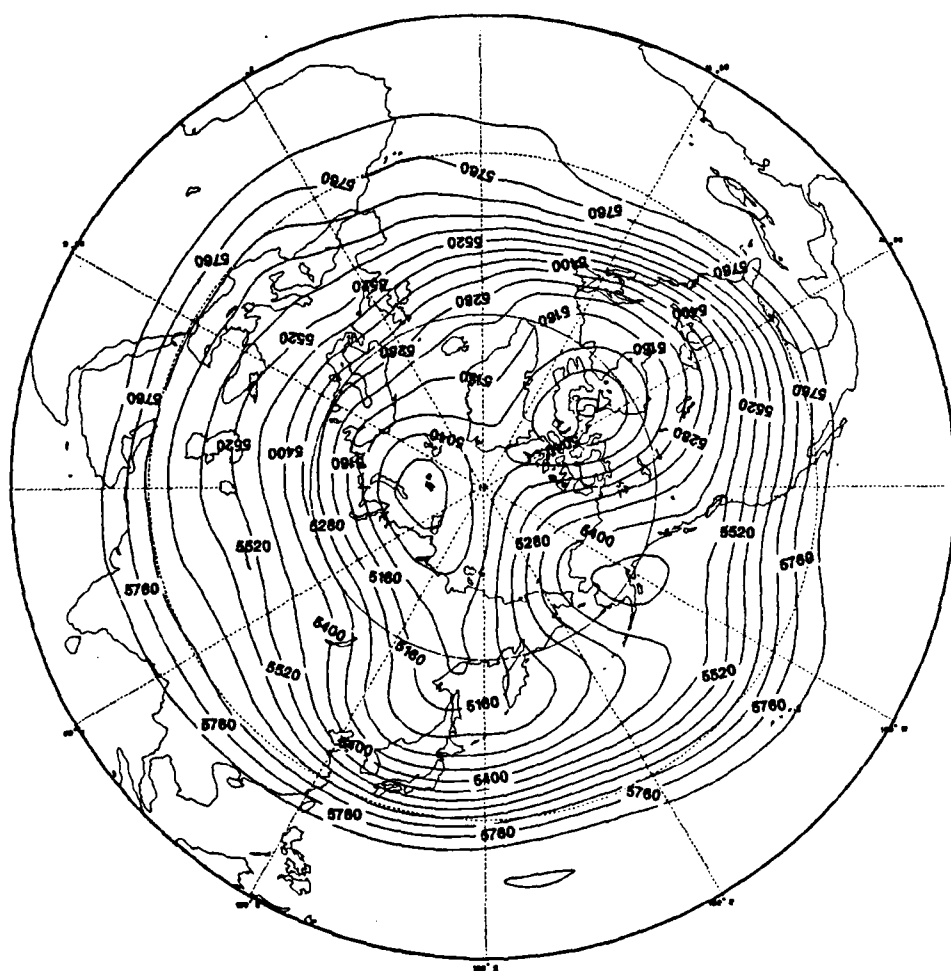


Figure 33. Polar Stereographic Plot of 500mb Average Height Field for December 1983

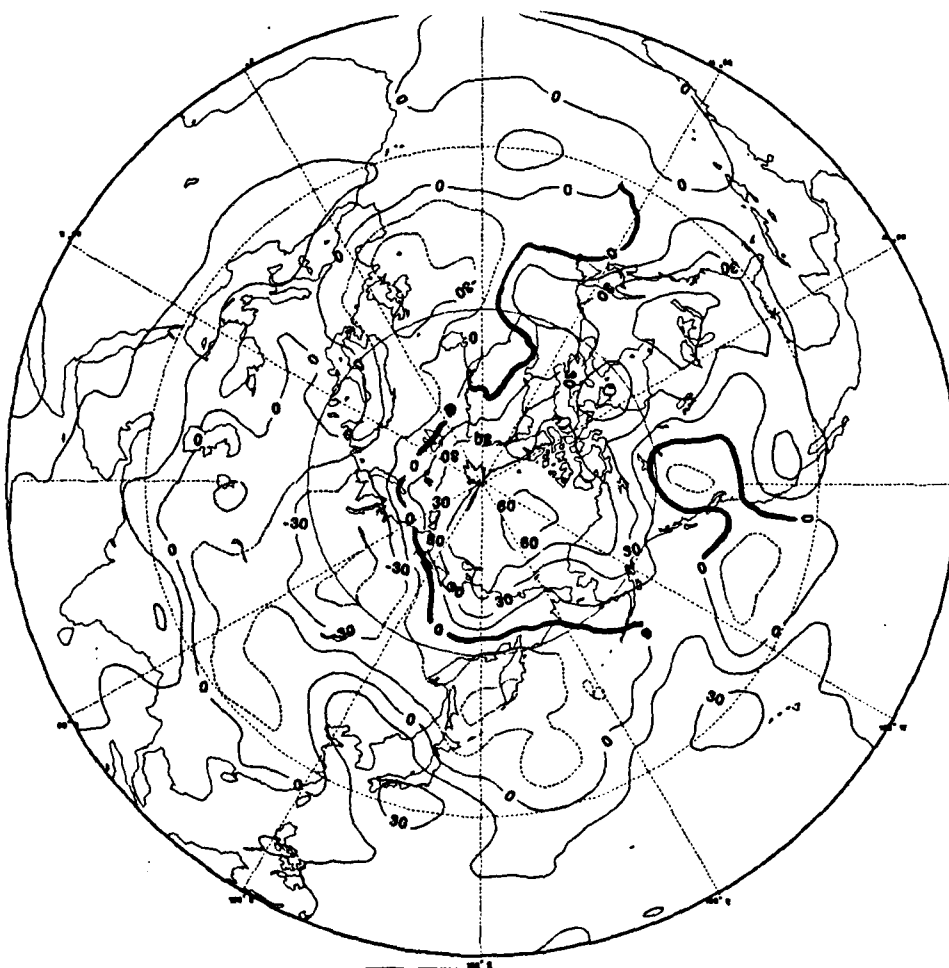


Figure 34. Polar Stereographic Plot of 48-hr Average Forecast Error for December 1983 (Contour Interval = 15 m)

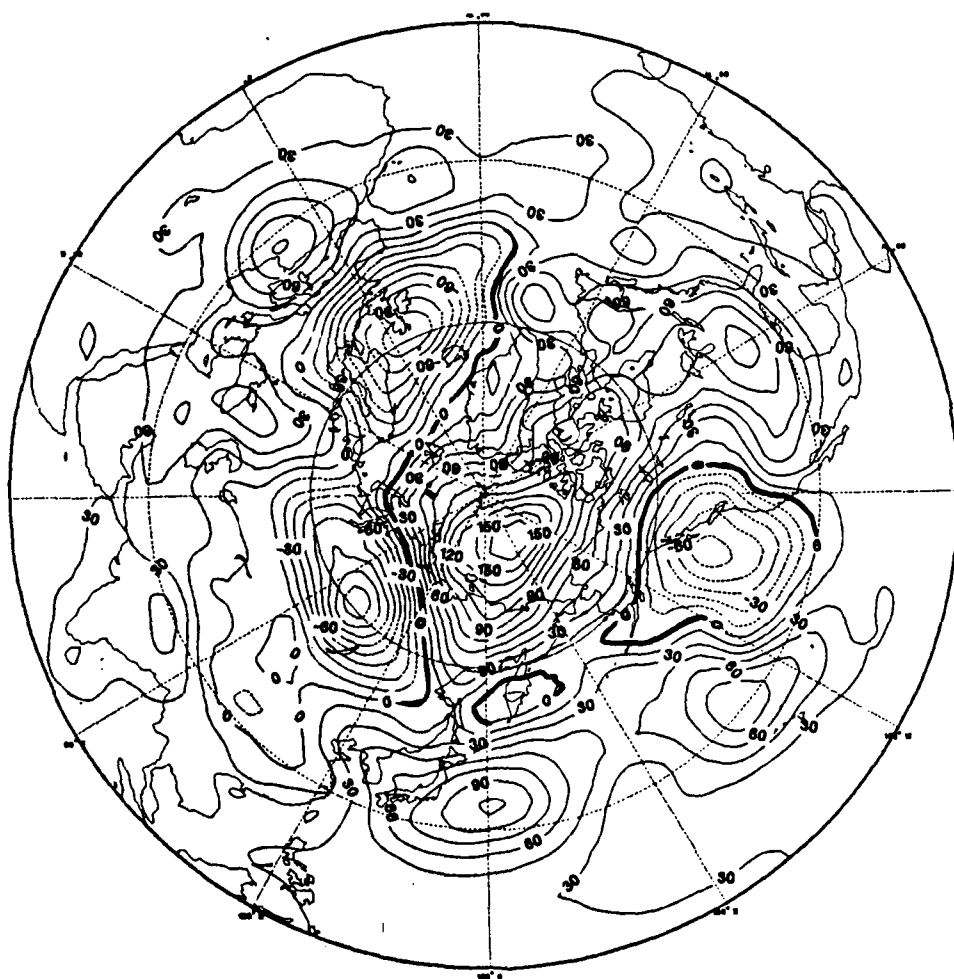


Figure 35. Polar Stereographic Plot of 96-hr Average  
Forecast Error for December 1983  
(Contour Interval = 15 m)

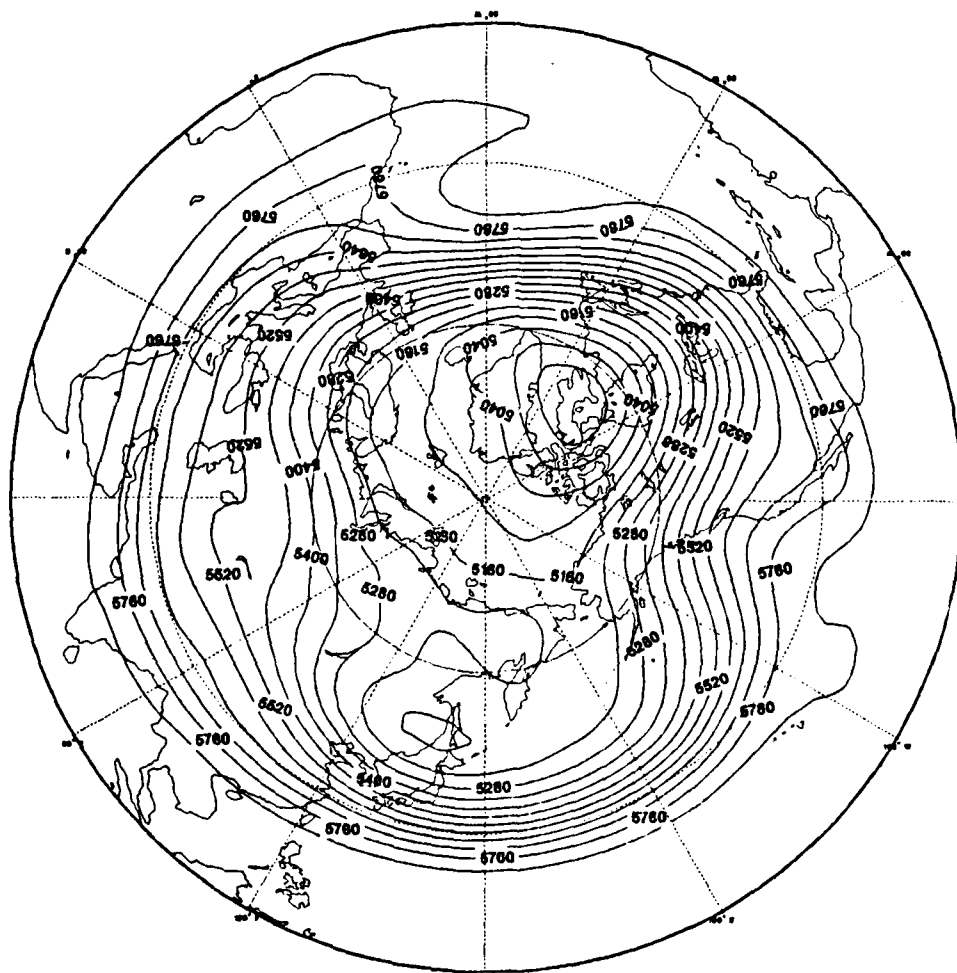


Figure 36. Polar Stereographic Plot of 500mb Average Height Field for January 1984 (Contour Interval = 60 m)

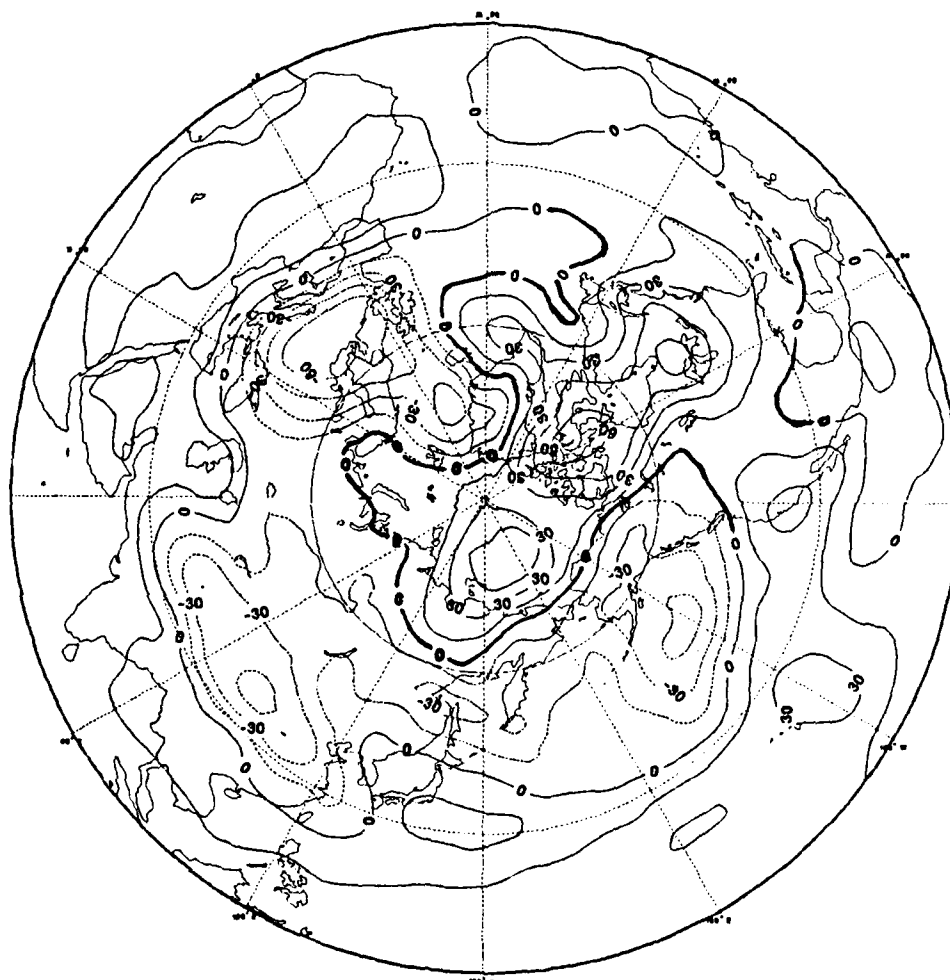


Figure 37. Polar Stereographic Plot of 48-hr Average Forecast Error for January 1984 (Contour Interval = 15 m)

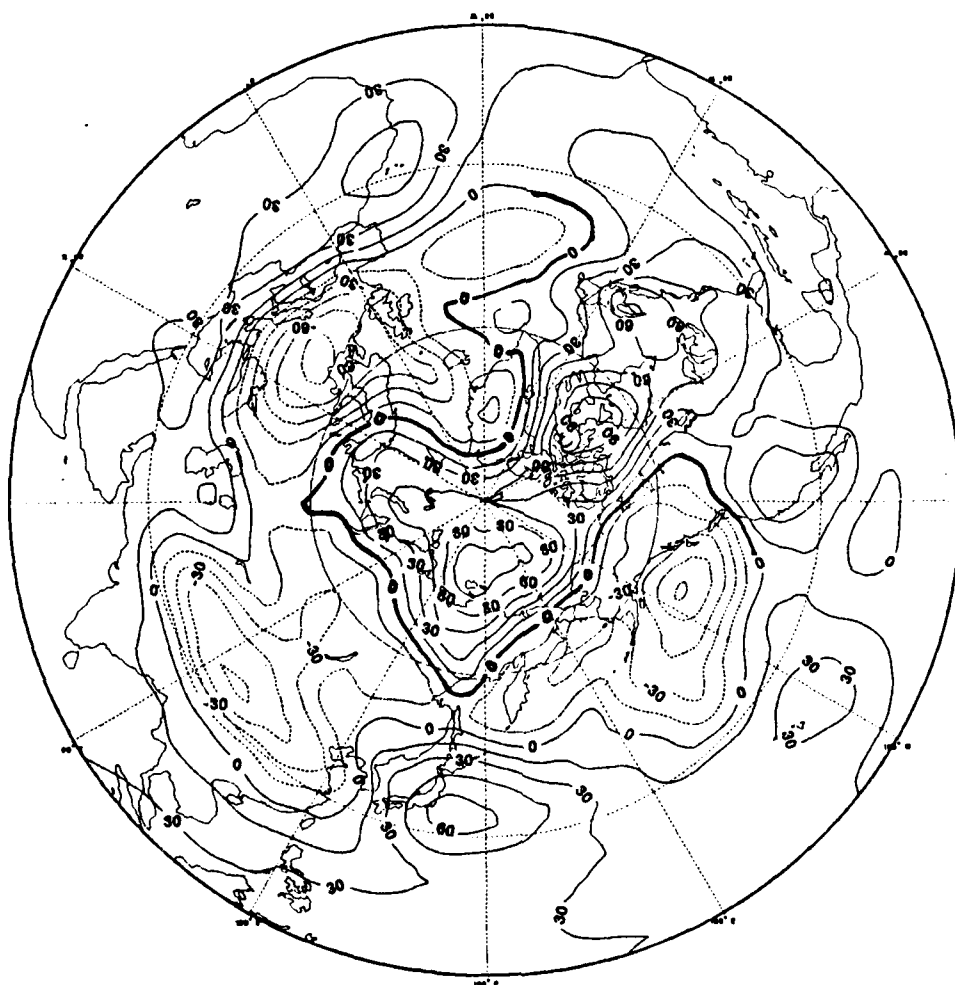


Figure 38. Polar Stereographic Plot of 96-hr Average Forecast Error for January 1984 (Contour Interval = 15 m)

# LIST OF REFERENCES

- Arakawa, A. and V.R. Lamb, 1977: Computational design of the basic dynamical processes of the UCLA general circulation model, Methods in Computational Physics, Vol. 17, Academic Press Inc., New York.
- Arakawa, A. and W.H. Schubert, 1974: Interaction of a cumulus cloud ensemble with the large-scale environment, Part 1., J. Atmos. Sci., 31, 687-701.
- Baumhefner, D. and P. Downey, 1978: Forecasts intercomparisons from three numerical weather prediction models, Bull. Amer. Meteor. Soc., 1245-1279.
- Bettge, T.W., 1981: An examination of the characteristics of planetary scale systematic forecast errors, Preprints of Fifth Conference on Numerical Weather Prediction, 109-114.
- Deardorff, J.W., 1972: Parameterization of the planetary boundary layer for use in general circulation models, Mon. Wea. Rev., 100, 93-106.
- Lambert, S.J. and P.E. Merilees, 1978: A study of planetary wave errors in a spectral numerical weather prediction model, Atmosphere-Ocean, 16, 197-211.
- Lord, S.J., 1978: Development and observational verification of a cumulus cloud parameterization, Ph.D. Thesis, Dept. of Atmos. Sci., UCLA.
- Miyakoda, K., G.D. Hembree, R.F. Strickler and I. Shulman, 1972: Cumulative results of extended forecast experiments. I. Model performance for winter cases, Mon. Wea. Rev., 100, 836-855.
- Morse, P.A., 1983: NOGAPS verification using spectral components, M.S. Thesis, Dept. of Meteorology, Naval Postgraduate School, Monterey, Ca.
- Rosmond, T.E., 1981: NOGAPS: Naval Operational Global Atmospheric Prediction System, Preprints of Fifth Conference on Numerical Weather Prediction, 74-79.
- Schlesinger, M.E., 1976: A numerical simulation of the general circulation of atmospheric ozone, Ph.D. Thesis, Dept. of Atmos. Sci., UCLA.

Somerville, R., 1980: Tropical influences on the predictability of ultralong waves, J. Atmos. Sci., 37, 1141-1156.

INITIAL DISTRIBUTION LIST

	No. Copies
1. Defense Technical Information Center Cameron Station Alexandria, VA 22314	2
2. Library, Code 0142 Naval Postgraduate School Monterey, CA 93943	2
3. Meteorology Reference Center, Code 63 Department of Meteorology Naval Postgraduate School Monterey, CA 93943	1
4. Professor Carlyle H. Wash, Code 63Cw Department of Meteorology Naval Postgraduate School Monterey, CA 93943	5
5. Professor James Boyle, Code 63Xj Department of Meteorology Naval Postgraduate School Monterey, CA 93943	1
6. Chairman, Code 68Mr Department of Oceanography Naval Postgraduate School Monterey, CA 93943	1
7. Chairman, Code 63Rd Department of Meteorology Naval Postgraduate School Monterey, CA 93943	1
8. Lcdr Robert C. Showalter Naval Eastern Oceanographic Center McAdie Bldg (U-117) Norfolk, VA 23511	3
9. Capt Peter A. Morse Det 4, 3rd Weather Squadron Holloman AFB, NM 88330	1
10. Director Naval Oceanography Division Naval Observatory 34th and Massachusetts Avenue NW Washington, D.C. 20390	1

11. Commander 1  
Naval Oceanography Command  
NSTL Station  
Bay St. Louis, MS 39522
12. Commanding Officer 1  
Naval Oceanographic Office  
NSTL Station  
Bay St. Louis, MS 39522
13. Commanding Officer 1  
Fleet Numerical Oceanography Center  
Monterey, CA 93940
14. Commanding Officer 1  
Naval Ocean Research and Development  
Activity  
NSTL Station  
Bay St. Louis, MS 39522
15. Commanding Officer 1  
Naval Environmental Prediction  
Research Facility  
Monterey, CA 93940
16. Chairman, Oceanography Department 1  
U.S. Naval Academy  
Annapolis, MD 21402
17. Chief of Naval Research 1  
800 N. Quincy Street  
Arlington, VA 22217
18. Office of Naval Research (Code 480) 1  
Naval Ocean Research and  
Development Activity  
NSTL Station  
Bay St. Louis, MS 39522
19. Commander (Air-370) 1  
Naval Air Systems Command  
Washington, D.C. 20360
20. Chief, Ocean Services Division 1  
National Oceanic and Atmospheric  
Administration  
8060 Thirteenth Street  
Silver Spring, MD 20910
21. Dr. Alan Weinstein 1  
Leader, Code 422  
Ocean Sciences Division  
Office of Naval Research  
Arlington, VA 22217

- |     |   |   |
|-----|---|---|
| 22. | Chief, Technical Procedures Branch<br>Meteorological Services Division<br>National Oceanic and Atmospheric<br>Administration<br>National Weather Service<br>Silver Spring, MD 20910 | 1 |
| 23. | Chief, Technical Services Division<br>United States Air Force<br>Air Weather Service (MAC)<br>Air Force Global Weather Central<br>Offutt AFB, NB 68113                              | 1 |
| 24. | Scientific Liaison Office<br>Office of Naval Research<br>Scripps Institution of Oceanography<br>La Jolla, CA 92037  | 1 |
| 25. | Library<br>Scripps Institution of Oceanography<br>P.O. Box 2367<br>La Jolla, CA 92037   | 1 |
| 26. | Library<br>Department of Oceanography<br>University of Washington<br>Seattle, WA 98105  | 1 |
| 27. | Library<br>CICESE<br>P.O. Box 4803<br>San Ysidro, CA 92073  | 1 |
| 28. | Library<br>School of Oceanography<br>Oregon State University<br>Corvallis, OR 97331   | 1 |
| 29. | Commander<br>Oceanographic Systems Pacific<br>Box 1390<br>Pearl Harbor, HI 96860  | 1 |